Chapter 1
Antennas

1.1 INTRODUCTION

An antenna is defined by Webster's Dictionary as "a usually metallic device (as a rod or wire) for radiating or receiving radio waves." The *IEEE Standard Definitions of Terms for Antennas* (IEEE Std 145-1973)* defines the antenna or aerial as "a means for radiating or receiving radio waves." In other words the antenna is the transitional structure between free-space and a guiding device, as shown in Figure 1.1. The guiding device or transmission line may take the form of a coaxial line or a hollow pipe (waveguide), and it is used to transport electromagnetic energy from the transmitting source to the antenna, or from the antenna to the receiver. In the former case we have a transmitting antenna and in the latter a receiving antenna.

In addition to receiving or transmitting energy, an antenna is usually required to *optimize* or *accentuate* the radiation energy in some directions and suppress it in others. *Thus the antenna must act as a directional device in addition to a probing device*. It must then take various forms to meet the particular need at hand, and it may be a piece of conducting wire, an aperture, an assembly of elements (array), a reflector, a lens, and so forth.

1.2 TYPES OF ANTENNAS

We will now introduce and briefly discuss some forms of the various antenna types in order to get a glance as to what will be encountered in the remainder of the book.

1.2.1 Wire Antennas

Wire antennas are familiar to the layman because they are seen virtually everywhere—on automobiles, buildings, ships, aircraft, spacecraft, and so on. There are various shapes of wire antennas such as a straight wire

IEEE Transactions on Antennas and Propagation, vols. AP-17, No. 3, May 1969 and AP-22, No. 1, January 1974.

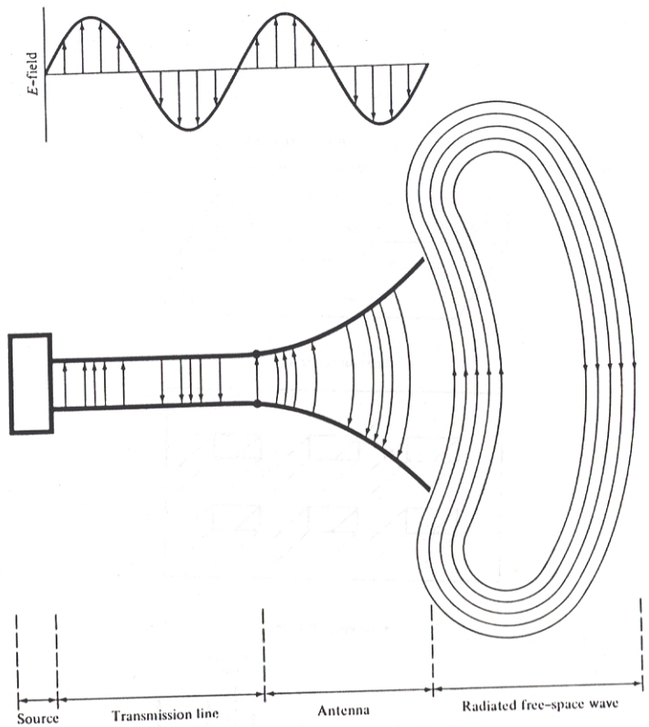

Figure 1.1 Antenna as a transition device.

(dipole), loop, and helix which are shown in Figure 1.2. Loop antennas need not only be circular. They may take the form of a rectangle, square, ellipse, or any other configuration. The circular loop is the most common because of its simplicity in construction.

1.2.2 Aperture Antennas

Aperture antennas may be more familiar to the layman today than in the past because of the increasing demand for more sophisticated forms of antennas and the utilization of higher frequencies. Some forms of aperture antennas are shown in Figure 1.3. Antennas of this type are very useful for aircraft or spacecraft applications, because they can be very conveniently

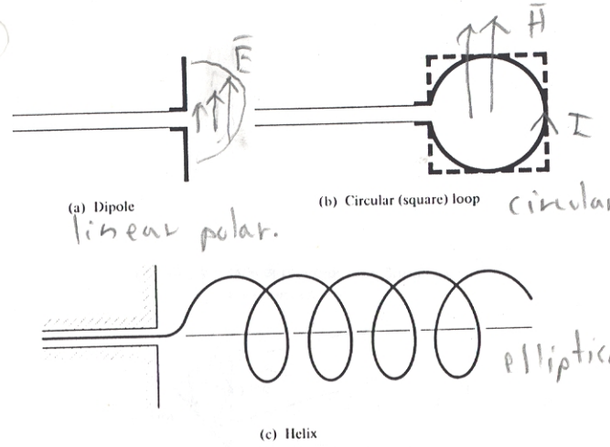

Figure 1.2 Wire antenna configurations.

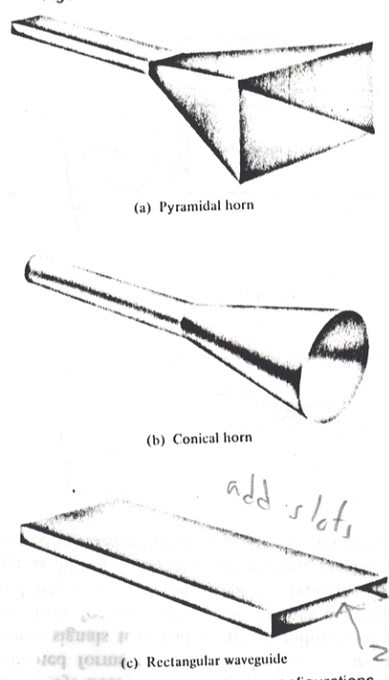

Figure 1.3 Aperture antenna configurations.

flush-mounted on the skin of the aircraft or spacecraft. In addition, they can be covered with a dielectric material to protect them from hazardous conditions of the environment.

1.2.3 Array Antennas

Many applications require radiation characteristics that may not be achievable by a single element. It may, however, be possible that an aggregate of radiating elements in an electrical and geometrical arrangement (an array) will result in the desired radiation characteristics. The arrangement of the array may be such that the radiation from the elements adds up to give a radiation maximum in a particular direction or directions, minimum in others, or otherwise as desired. Typical examples of arrays are shown in Figure 1.4. Usually the term *array* is reserved for an arrangement in which the individual radiators are separate as shown in Figures 1.4(a) and (b). However the same term is also used to describe an assembly of radiators mounted on a continuous structure, shown in Figure 1.4(c).

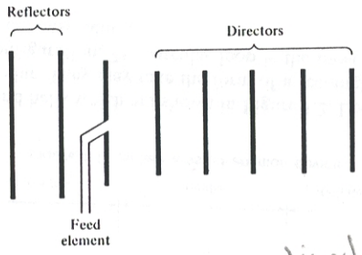

(a) Yagi-Uda array

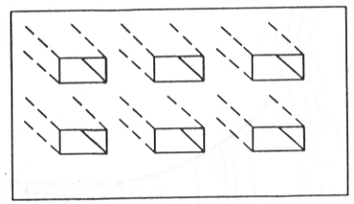

(b) Aperture array

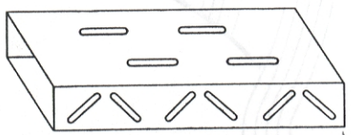

(c) Slotted-waveguide array

Figure 1.4 Typical wire and aperture array configurations.

1.2.4 Reflector Antennas

The success in the exploration of outer space has resulted in the advancement of antenna theory. Because of the need to communicate over great distances, sophisticated forms of antennas had to be used in order to transmit and receive signals that had to travel millions of miles. A very common antenna form for such an application is a parabolic reflector shown in Figures 1.5(a) and (b). Antennas of this type have been built with diameters as large as 305 m. Such large dimensions are needed to achieve the high gain required to transmit or receive signals after millions of miles of

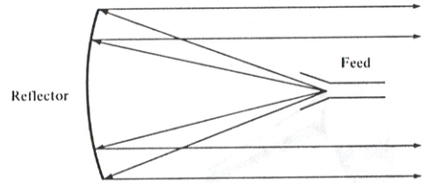

(a) Parabolic reflector with front feed

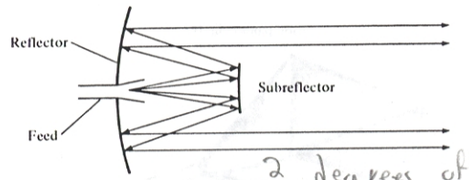

(b) Parabolic reflector with Cassegrain feed

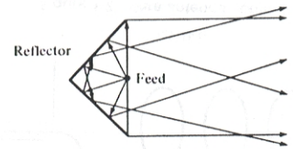

(c) Corner reflector

Figure 1.5 Typical reflector configurations.

travel. Another form of a reflector, although not as common as the parabolic, is the corner reflector, shown in Figure 1.5(c).

1.2.5 Lens Antennas

Lenses are primarily used to collimate incident divergent energy to prevent it from spreading in undesired directions. By properly shaping the geometrical configuration and choosing the appropriate material of the lenses, they can transform various forms of divergent energy into plane waves. They can be used in most of the same applications as are the parabolic reflectors, especially at higher frequencies. Their dimensions and weight become exceedingly large at lower frequencies. Lens antennas are classified according to the material from which they are constructed, or according to their geometrical shape. Some forms are shown in Figure 1.6.

In summary, an ideal antenna is one that will radiate all the power delivered to it from the transmitter in a desired direction or directions. In practice, however, such ideal performances cannot be achieved but may be closely approached. Various types of antennas are available and each type can take different forms in order to achieve the desired radiation characteristics for the particular application.

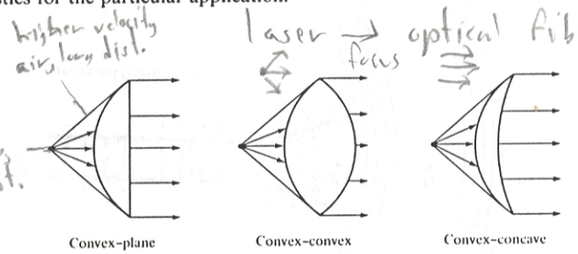

(a) Lens antennas with index of refraction $n > 1$

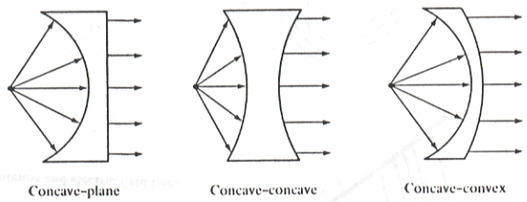

(b) Lens antennas with index of refraction $n < 1$

Figure 1.6 Typical lens antenna configurations. (SOURCE: L. V. Blake, *Antennas*, Wiley, New York, 1966).

1.3 RADIATION MECHANISM

One of the first questions that may be asked concerning antennas would be "how is radiation accomplished?" In other words, how are the electromagnetic fields generated by the source, contained and guided within the transmission line and antenna, and finally "detached" from the antenna to form a free-space wave? The best explanation may be given by an illustration.

Let us consider a voltage source connected to a two-conductor transmission line which is connected to an antenna. This is shown in Figure 1.7(a). Applying a voltage across the two-conductor transmission line creates an electric field between the conductors. The electric field has associated with it electric lines of force which are tangent to the electric field at each point and their strength is proportional to the electric field intensity. The electric lines of force have a tendency to act on the free electrons (easily detachable from the atoms) associated with each conductor and force them to be displaced. The movement of the charges creates a current that in turn creates a magnetic field intensity. Associated with the magnetic field intensity are magnetic lines of force which are tangent to the magnetic field.

We have accepted that electric field lines start on positive charges and end on negative charges. They also can start on a positive charge and end at infinity, start at infinity and end on a negative charge, or form closed loops neither starting or ending on any charge. Magnetic field lines always form closed loops encircling current-carrying conductors because there are no magnetic charges. In some mathematical formulations, it is often convenient to introduce magnetic charges and magnetic currents to draw a parallel between solutions involving electric and magnetic sources.

The electric field lines drawn between the two conductors help to exhibit the distribution of charge. If we assume that the voltage source is sinusoidal, we expect the electric field between the conductors to also be sinusoidal with a period equal to that of the applied source. The relative magnitude of the electric field intensity will be indicated by the density (bunching) of the lines of force with the arrows showing the relative direction (positive or negative). The creation of time-varying electric and magnetic fields between the conductors forms electromagnetic waves which travel along the transmission line, as shown in Figure 1.7(a). The electromagnetic waves enter the antenna and have associated with them electric charges and corresponding currents. If we remove part of the antenna structure, as shown in Figure 1.7(b), free-space waves can be formed by "connecting" the open ends of the electric lines (shown dashed). The free-space waves are also periodic but a constant phase point P_0 moves outwardly with the speed of light and travels a distance of $\lambda/2$ (to P_1) in the time of one-half of a period. It has been shown [2] that close to the antenna the constant phase point P_0 moves faster than the speed of light but approaches the speed of light at points far away from the antenna (analogous to phase velocity inside a rectangular waveguide). Figure 1.8 displays

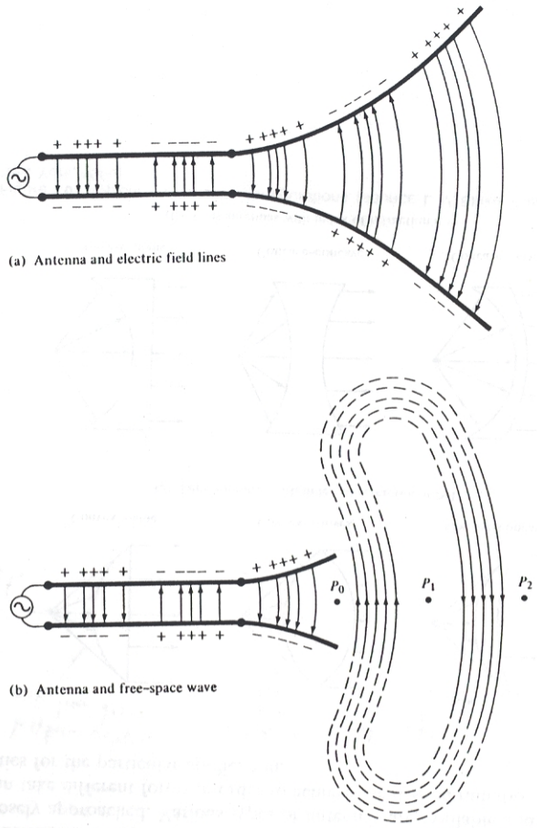

Figure 1.7 Source, transmission line, antenna, and detachment of electric field lines.

the creation and travel of free-space waves by a prolate spheroid with $\lambda/2$ interfocal distance where λ is the wavelength. The free-space waves of a center-fed $\lambda/2$ dipole, except in the immediate vicinity of the antenna, should essentially be the same as those of the prolate spheroid.

The question still unanswered is how the guided waves are detached from the antenna to create the free-space waves that are indicated as closed loops in Figures 1.7 and 1.8. Before we attempt to explain that, let us draw a parallel between the guided and free-space waves, and water waves [3]

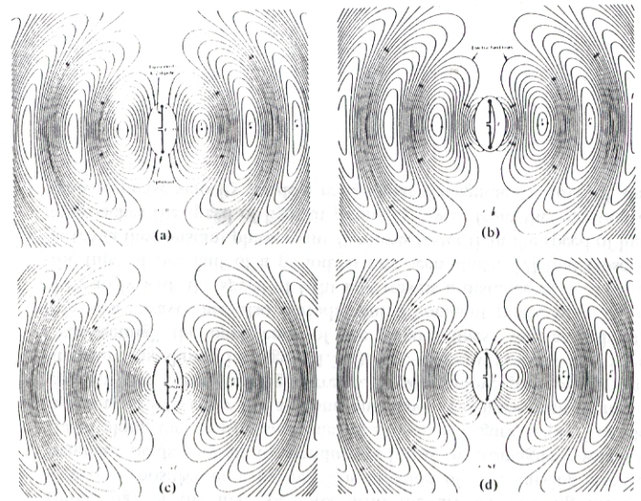

Figure 1.8 Electric field lines of free-space wave for a $\lambda/2$ antenna at $t=0$, $T/8$, $T/4$, and $3T/8$. (SOURCE: J. D. Kraus and K. R. Carver, *Electromagnetics*, 2nd ed., McGraw-Hill, New York, 1973. Reprinted with permission of J. D. Kraus and John D. Cowan, Jr.)

spherical waves

created by the dropping of a pebble in a calm body of water or initiated in some other manner. Once the disturbance in the water has been initiated, water waves are created which begin to travel outwardly. If the disturbance has been removed, the waves do not stop or extinguish themselves but continue their course of travel. If the disturbance persists, new waves are continuously created which lag in their travel behind the others. The same is true with the electromagnetic waves created by an electric disturbance. If the initial electric disturbance by the source is of a short duration, the created electromagnetic waves will travel inside the transmission line, then into the antenna, and finally will be radiated as free-space waves, even if the electric source has ceased to exist (as was with the water waves and their generating disturbance). If the electric disturbance is of a continuous nature, electromagnetic waves will exist continuously and follow in their travel behind the others. This is shown in Figure 1.9 for a biconical antenna. When the electromagnetic waves are within the transmission line and antenna, their existence is associated with the presence of the charges inside the conductors. However, when the waves are radiated, they form closed loops and there are no charges to sustain their existence. *This leads us to conclude that electric charges are required to excite the fields but are not*

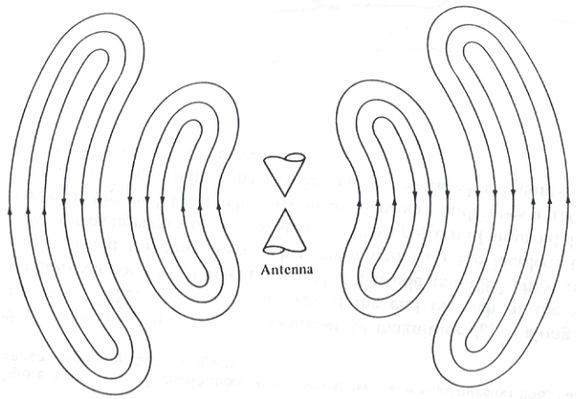

Figure 1.9 Electric field lines of free-space wave for biconical antenna.

needed to sustain them and may exist in their absence. This is in direct analogy with water waves.

Now let us attempt to explain the mechanism by which the electric lines of force are detached from the antenna to form the free-space waves. This will again be illustrated by an example of a small antenna where the time of travel is negligible. This is only necessary to give a better physical interpretation of the detachment of the lines of force. Although a somewhat simplified mechanism, it does allow one to visualize the creation of the free-space waves. Figure 1.10(a) displays the lines of force created between the arms of a small center-fed dipole in the first quarter of the period during which time the charge has reached its maximum value (assuming a sinusoidal time variation) and the lines have traveled outwardly a radial distance $\lambda/4$. For this example, let us assume that the number of lines formed are three. During the next quarter of the period, the original three lines travel an additional $\lambda/4$ (a total of $\lambda/2$ from the initial point) and the charge density on the conductors begins to diminish. This can be thought of as being accomplished by introducing opposite charges which at the end of the first half of the period have neutralized the charges on the conductors. The lines of force created by the opposite charges are three and travel a distance $\lambda/4$ during the second quarter of the first half, and they are shown dashed in Figure 1.10(b). The end result is that there are three lines of force pointed upward in the first $\lambda/4$ distance and the same number of lines directed downward in the second $\lambda/4$. Since there is no net charge on the antenna, then the lines of force must have been forced to detach themselves from the conductors and to unite together to form closed loops. This is shown in Figure 1.10(c). In the remaining second half of the period, the same

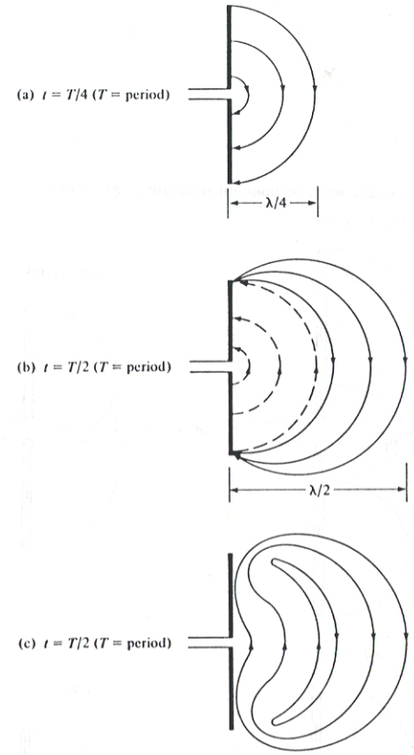

Figure 1.10 Formation and detachment of electric field lines for short dipole.

procedure is followed but in the opposite direction. After that, the process is repeated and continues indefinitely.

1.4 CURRENT DISTRIBUTION ON A THIN WIRE ANTENNA

In the preceding section we discussed the movement of the free electrons on the conductors representing the transmission line and the antenna. In order to illustrate the creation of the current distribution on a linear dipole, and its subsequent radiation, let us first begin with the geometry of a lossless two-wire transmission line, as shown in Figure 1.11(a). The movement of the

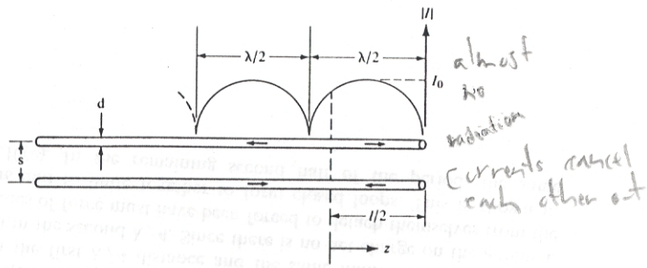

(a) Two-wire transmission line

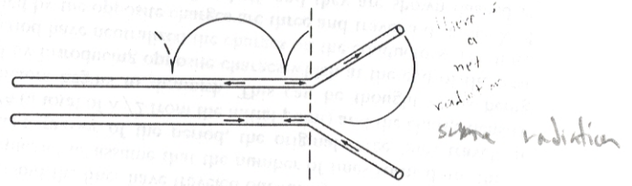

(b) Flared transmission line

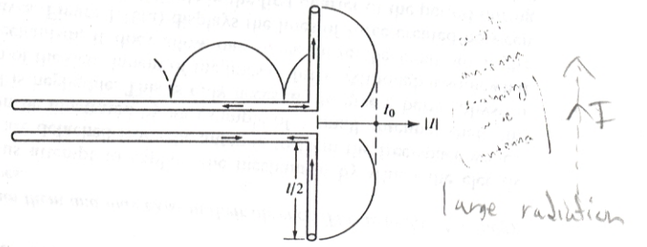

(c) Linear dipole

Figure 1.11 Current distribution on a lossless two-wire transmission line, flared transmission line, and linear dipole.

charges creates a traveling wave current, of magnitude $I_0/2$, along each of the wires. When the current arrives at the end of each of the wires, it undergoes a complete reflection (equal magnitude and 180° phase reversal). The reflected traveling wave, when combined with the incident traveling wave, forms in each wire a pure standing wave pattern of sinusoidal form as shown in Figure 1.11(a). The current in each wire undergoes a 180° phase reversal between adjoining half cycles. This is indicated in Figure 1.11(a) by the reversal of the arrow direction.

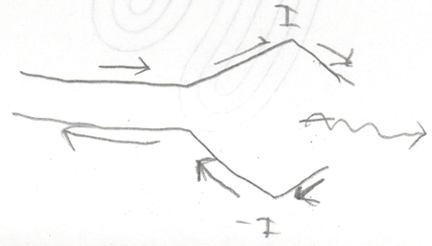

For the two-wire balanced (symmetrical) transmission line, the current in a half-cycle of one wire is of the same magnitude but 180° out-of-phase from that in the corresponding half-cycle of the other wire. If in addition the spacing between the two wires is very small ($s \ll \lambda$), the fields radiated by the current of each wire are essentially cancelled by those of the other. The net result is an almost ideal (and desired) nonradiating transmission line.

As the section of the transmission line between $0 \le z \le l/2$ begins to flare, as shown in Figure 1.11(b), it can be assumed that the current distribution is essentially unaltered in form in each of the wires. However, because the two wires of the flared section are not necessarily close to each other, the fields radiated by one do not necessarily cancel those of the other. Therefore there is a net radiation by the system.

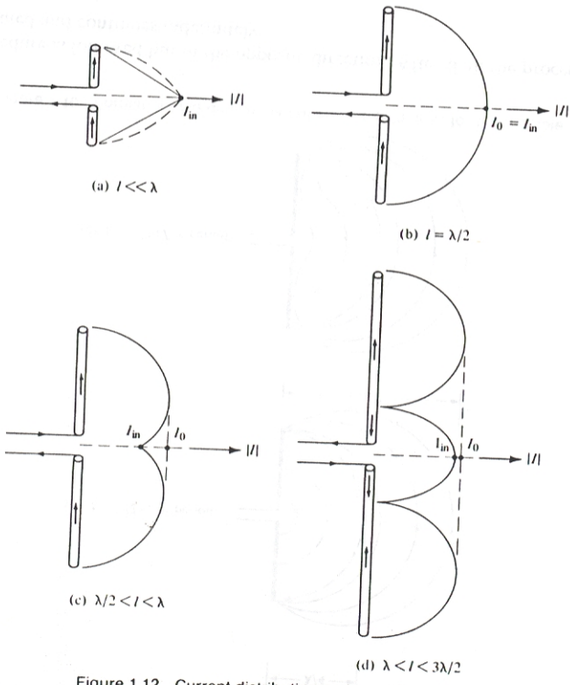

(a) $l \ll \lambda$

(b) $l = \lambda/2$

(c) $\lambda/2 < l < \lambda$

(d) $\lambda < l < 3\lambda/2$

Figure 1.12 Current distribution on linear dipoles.

Ultimately the flared section of the transmission line can take the form shown in Figure 1.11(c). This is the geometry of the widely used dipole antenna. Because of the standing wave current pattern, it is also classified as a standing wave antenna (as contrasted to the traveling wave antennas which will be discussed in detail in Chapter 9). If $l<\lambda$, the phase of the current standing wave pattern in each arm is the same throughout its length. In addition, spatially it is oriented in the same direction as that of the other arm as shown in Figure 1.11(c). Thus the fields radiated by the two arms of the dipole (vertical parts of a flared transmission line) will primarily reinforce each other toward most directions of observation (the phase due to the relative position of each small part of each arm must also be included for a complete description of the radiation pattern formation).

If the diameter of each wire is very small ($d \ll \lambda$), the ideal standing wave pattern of the current along the arms of the dipole is sinusoidal with a null at the end. However, its overall form depends on the length of each arm. For center-fed dipoles with $l \ll \lambda$, $l=\lambda/2$, $\lambda/2<l<\lambda$ and $\lambda<l<3\lambda/2$, the current patterns are illustrated in Figures 1.12(a)–(d). The current pattern of a very small dipole (usually $\lambda/50<l\leq\lambda/10$) can be approximated by a triangular distribution since $\sin(kl/2)\simeq kl/2$ when $kl/2$ is very small. This is illustrated in Figure 1.12(a).

Because of its cyclical spatial variations, the current standing wave pattern of a dipole longer than $\lambda(l>\lambda)$ undergoes 180° phase reversals between adjoining half-cycles. Therefore the current in all parts of the dipole does not have the same phase. This is demonstrated graphically in Figure 1.12(d) for $\lambda<l<3\lambda/2$. In turn, the fields radiated by some parts of the dipole will not reinforce those of the others. As a result, significant

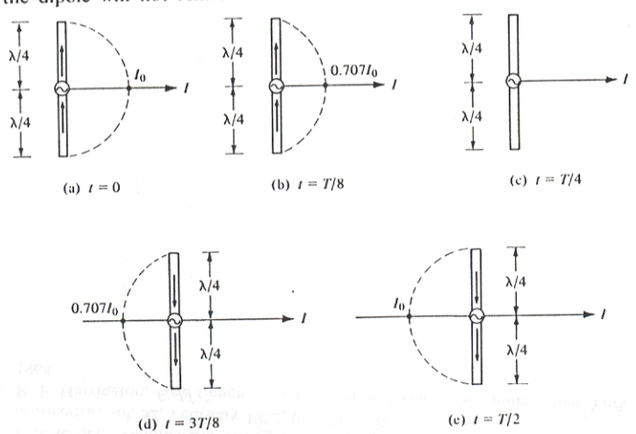

Figure 1.13 Current distribution on a $\lambda/2$ wire antenna for different times.

interference and cancelling effects will be noted in the formation of the total radiation pattern.

For a time-harmonic varying system of radian frequency $\omega=2\pi f$, the current standing wave patterns of Figure 1.12 represent the maximum current excitation for any time. The current variations, as a function of time, on a $\lambda/2$ center-fed dipole are shown in Figure 1.13 for $0\leq t\leq T/2$ where T is the period. These variations can be obtained by multiplying the current standing wave pattern of Figure 1.12(b) by $\cos(\omega t)$.

1.5 HISTORICAL ADVANCEMENT

The history of radio antennas began as early as 1887 with the first design taking the form of a loop. It was not until 1901 that Marconi used an array of 50 copper wires to perform the first transatlantic transmission. The greatest advancement of antenna theory and design was accomplished during World War II with the introduction of microwave antennas taking the form of reflectors, apertures, and arrays. Most of this work was later included in a classic book [4] edited by S. Silver. Considerable refinement in the theory of linear wire antennas was accomplished by R. W. P. King [5] and his associates at the Gordon McKay Laboratory of Harvard University. J. D. Kraus of Ohio State University introduced the helical antenna and much of his work is included in his classic book [6]. S. K. Schelkunoff of Bell Laboratories was able to provide mathematical formulations representing the radiation mechanisms of many antennas. His accomplishments bridged the gap between theory and experiment and provided better understanding of antennas [3].

With the introduction and advancement of computer techniques, antenna theory was again revived. Many mathematically intractable problems were now solved using numerical techniques. Advancements resulted from the introduction and application of the Geometrical Theory of Diffraction [7] and the Moment Method [8]. It is believed that the Geometrical Theory of Diffraction (which is most suitable for electrically large bodies), and the Moment Method (which is most suitable for electrically small bodies), today provide the two most promising analytical methods in antenna theory and design. The revival of the Geometrical Theory of Diffraction was primarily instrumented by the work of J. B. Keller and his associates at New York University in the 1950s. The introduction of the Moment Method to antenna theory resulted primarily from the work of R. F. Harrington at Syracuse University in the 1960s.

References

1. L. V. Blake, *Antennas*, Wiley, New York, 1966, p. 289.
2. J. D. Kraus and K. R. Carver, *Electromagnetics*, McGraw-Hill, New York, 1973, pp. 648–650.

3. S. K. Schelkunoff and H. T. Friis, *Antennas: Theory and Practice*, Wiley, New York, 1952.
4. S. Silver (ed.), *Microwave Antenna Theory and Design*, M. I. T. Radiation Laboratory Series, vol. 12, McGraw-Hill, New York, 1949.
5. R. W. P. King, *Theory of Linear Antennas*, Harvard University Press, Cambridge, Mass., 1956.
6. J. D. Kraus, *Antennas*, McGraw-Hill, New York, 1950.
7. J. B. Keller, "Geometrical Theory of Diffraction," *Journal of the Optical Society of America*, vol. 52, February 1962, pp. 116–130.
8. R. F. Harrington, *Field Computation by Moment Methods*, Macmillan, New York, 1968.

Chapter 2
Fundamental Parameters of Antennas

2.1 INTRODUCTION

To describe the performance of an antenna, definitions of various parameters are necessary. Some of the parameters are interrelated and not all of them need be specified for complete description of the antenna performance. Parameter definitions will be given in this chapter. Those in quotation marks will be from the *IEEE Standard Definitions of Terms for Antennas* (IEEE Std 145-1973).*

2.2 RADIATION PATTERN

An antenna *radiation pattern* is defined as "a graphical representation of the radiation properties of the antenna as a function of space coordinates. In most cases, the radiation pattern is determined in the far-field region and is represented as a function of the directional coordinates. Radiation properties include radiation intensity, field strength, phase or polarization." The radiation property of most concern is the three-dimensional spatial distribution of radiated energy as a function of the observer's position along a constant radius. A convenient set of coordinates is shown in Figure 2.1. A trace of the received power at a constant radius is called the *power pattern*. On the other hand, a graph of the spatial variation of the electric (or magnetic) field along a constant radius is called a *field pattern*. In practice, the three-dimensional pattern is measured and recorded in a series of two-dimensional patterns. However, for most practical applications, a few

IEEE Transactions on Antennas and Propagation, vols. AP-17, No. 3, May 1969; AP-22, No. 1, January 1974; and AP-31, No. 6, Part II, November 1983.

LECTURE 30

Radiation

The system that acts as the transition or matching unit between the source and waves in space → radiator/antenna

Important Antenna Information

(1) Relative field strength for various directions (antenna pattern) directivity
(2) Total radiated power for a specific voltage/current excitation
(3) Input impedance of radiator (matching)
(4) Bandwidth of antenna
(5) Radiation efficiency = $P_{radiated}/P_{total}$ metal, dielectric loss
(6) Max field strengths that may cause corona or dielectric breakdown

Types of Antennas

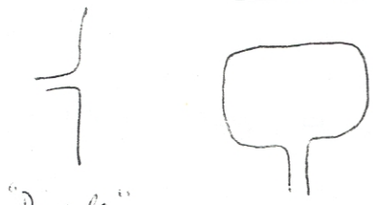

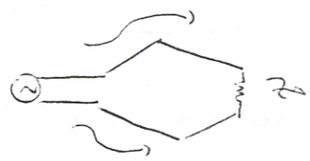

"Traveling wave"

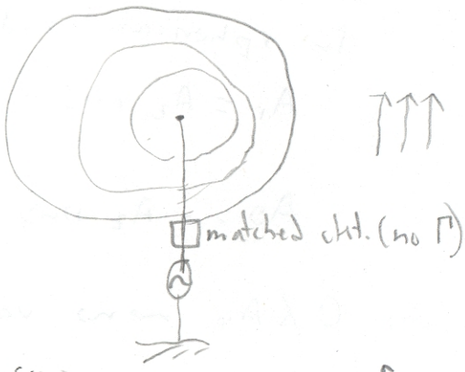

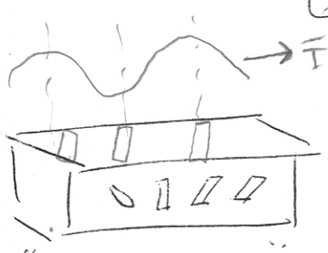

"Slot array"

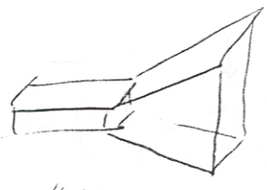

"Horn Antenna"

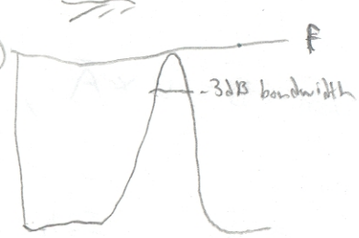

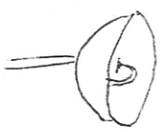

Parabolic Antenna

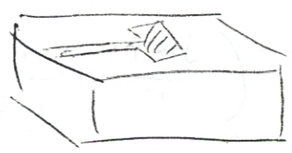

"Patch Antenna"

→ Hertzian Dipole

Antenna's length $h \ll \lambda$ $h < \frac{\lambda}{50}$

The current varies sinusoidally with time only

$$I = I_0 e^{j\omega t}$$ no space dependence

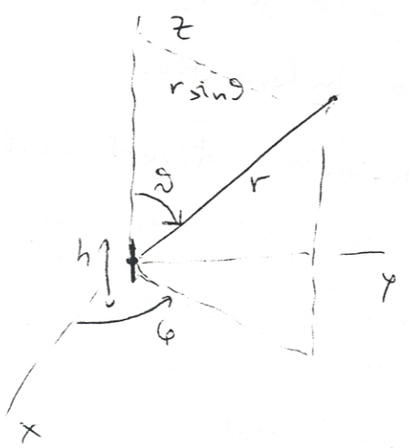

&

For any point at radius r, the retarded potential $\bar{A}$ is:

R = dist. from pt. to any pt. on dipole

$$\bar{A} = \mu \int_V \frac{\bar{J} e^{-jkR}}{4\pi R} dv'$$

$$= \mu \frac{h I_0}{4\pi r} e^{-j\left(\frac{\omega}{v} r\right)}$$

In spherical coords:

$$A_r = A_z \cos\theta = \mu \frac{I_0}{4\pi r} e^{-jkr} \cos\theta$$

$$A_\theta = -A_z \sin\theta = -\mu \frac{I_0}{4\pi r} e^{-jkr} \sin\theta \qquad , \quad k = \frac{\omega}{v} = \omega\sqrt{\mu\varepsilon}$$

$A_\phi = 0$ & $A_\phi \sim$ no variation with ϕ, due to ϕ-symmetry

$$\bar{H} = \bar{B} = \nabla \times \bar{A} \quad , \quad \bar{E} = -\frac{j\omega}{k^2} \nabla(\nabla \cdot \bar{A}) - j\omega\bar{A}$$

$$\downarrow$$

$$H_\phi = \frac{I_0 h}{4\pi} e^{-jkr} \left(\frac{jk}{r} + \frac{1}{r^2}\right) \sin\theta$$

$$E_r = \frac{I_0 h}{4\pi} e^{-jkr} \left(\frac{2\eta}{r^2} + \frac{2}{j\omega\varepsilon r^3}\right) \cos\theta$$

$$E_\theta = \frac{I_0 h}{4\pi} e^{-jkr} \left(\frac{j\omega\mu}{r} + \frac{1}{j\omega\varepsilon r^3} + \frac{\eta}{r^2}\right) \sin\theta$$

Near-field ($r \ll$) $\frac{1}{r^3} \gg \frac{1}{r^2} \gg \frac{1}{r}$ antenna + ICs

$H_\varphi \sim 1/r^2$ Never have plane wave

$E_r, E_\vartheta \sim 1/r^3$ (90° difference)

Far-field ($r \gg$) $\frac{1}{r} \gg \frac{1}{r^2} \gg \frac{1}{r^3}$ keep

$$H_\varphi \simeq \frac{jk I_0 h}{4\pi r} (\sin\vartheta) e^{-jkr}$$

$$E_\vartheta \simeq \frac{j\omega\mu I_0 h}{4\pi r} (\sin\vartheta) e^{-jkr} = \eta H_\varphi$$

$E_r \approx 0$, $H_r \approx 0$] plane/TEM wave

} Uniform plane wave

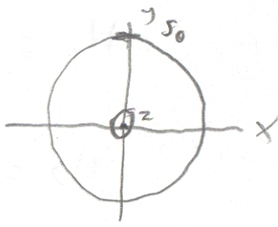

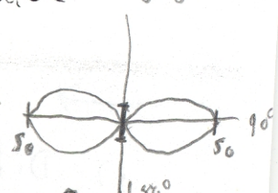

max pwr. density $\sim \frac{1}{r^2}$

$S_0 \sin^2\theta$ (W/m^2)

$\hat{r}$ direction

radiation normal to ant.

like donut

medium of propagation

Power density $P_r = \frac{1}{2}\mathrm{Re}(\underbrace{E \times H^*}_{\hat{r}}) = \frac{\eta k^2 I_0^2 h^2}{32\pi^2 r^2} \sin^2\vartheta = S(r,\theta)$ (η: medium prop.) $k = \frac{2\pi}{\lambda}$

Total power:

$$W = \oint_S \bar{P}\cdot d\bar{s} = \int_0^\pi P_r \underbrace{2\pi r^2 \sin\vartheta\, d\vartheta}_{ds} = \frac{\eta\pi I_0^2}{3}\left(\frac{h}{\lambda}\right)^2$$

★ independent of r

Watts

Norm. Rad. Intensity $F(\theta) = \frac{S(R,\theta,\phi)}{S_0} = \sin^2\theta$ (R: sphere of radius r)

For air: $\eta = 120\pi \Rightarrow W \cong 40\pi^2 I_0^2 \left(\frac{h}{\lambda}\right)^2$ Watts

Magnetic Dipole ≡ Current Loop

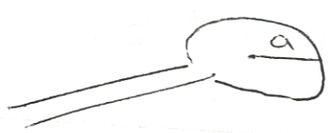

Small current loop of radius a and current I

Duality: $\bar{H} \to \bar{E}$, $-\bar{E} \to \bar{H}$, $\mu \leftrightarrow \varepsilon$

$I\pi a^2 \overset{\text{dual}}{\Longleftrightarrow} qh = I_0 h/j\omega$

Mag. Dipole — Fe. Dipole

$I_0 = \frac{dq}{dt} \xrightarrow{\text{phasor}} j\omega q = I_0$

$$E_\varphi = -\frac{j\omega\mu_1 I a^2}{4} e^{-jkr}\left(\frac{jk}{r}+\frac{1}{r^2}\right)\sin\vartheta$$

$$H_r = \frac{j\omega\mu_1 I a^2}{4} e^{-jkr}\left(\frac{2}{\eta r^2}+\frac{2}{j\omega\mu_1 r^3}\right)\cos\vartheta$$

$$H_\vartheta = \frac{j\omega\mu_1 I a^2}{4} e^{-jkr}\left(\frac{j\omega\varepsilon}{r}+\frac{1}{j\omega\mu_1 r^3}+\frac{1}{\eta r^2}\right)\sin\vartheta$$

Assumptions for Far-Field

1) Differences in radius vector to different points of the radiator are unimportant in their effect on magnitudes, but very important on phases

2) ~~Decrease~~ components decreasing faster than $1/r$ are negligible compared to those $\sim 1/r$

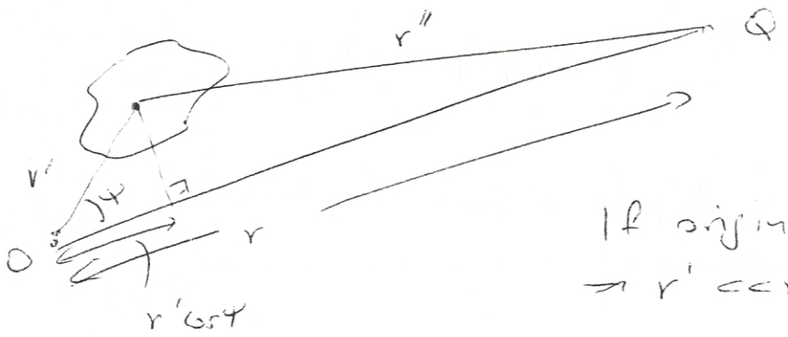

$$\bar{A} = \mu \int_V \frac{\bar{J} e^{-jkr''}}{4\pi r''} dV'$$

If origin close to the antenna

$\Rightarrow r' \ll r \Rightarrow$

$$\Rightarrow r'' = \sqrt{r^2 + r'^2 - 2rr'\cos\psi} \simeq r - r'\cos\psi$$

$$\bar{A} = \mu \frac{e^{-jkr}}{4\pi r} \underbrace{\int_{V'} \bar{J}\, e^{jkr'\cos\psi} dV'}_{\text{radiation vector } \bar{N}}$$

Only a function of the assumed current distribution and the direction ψ between r, r'

$$\bar{A} = \mu \frac{e^{-jkr}}{4\pi r}\bar{N} = \mu \frac{e^{-jkr}}{4\pi r}(\hat{r}N_r + \hat{\vartheta}N_\vartheta + \hat{\varphi}N_\varphi)$$

$$\bar{B} = \nabla \times \bar{A} \xrightarrow{\text{Sph. Coords.}}$$

$$H_\theta = -\frac{1}{\mu r}\frac{\partial}{\partial r}(rA_\phi) = \frac{jk}{4\pi r} e^{-jkr} N_\phi$$

$$H_\phi = \frac{1}{\mu r}\frac{\partial}{\partial r}(rA_\theta) = -\frac{jk}{4\pi r} e^{-jkr} N_\theta$$

and

$$E_\theta = -\frac{j\omega\mu}{4\pi r} e^{-jkr} N_\theta \,, \quad E_\phi = -\frac{j\omega\mu}{4\pi r} e^{-jkr} N_\phi$$

Poynting: $P_r = \frac{1}{2} Re\,(E_\theta H_\phi^* - E_\phi H_\theta^*) = \frac{\eta}{8\lambda^2 r^2}\left[|N_\theta|^2 + |N_\phi|^2\right]$

$$W = \int_0^\pi \int_0^{2\pi} P_r r^2 \sin\theta \, d\theta \, d\phi = \frac{\eta}{8\lambda^2} \int_0^\pi \int_0^{2\pi} \left[|N_\theta|^2 + |N_\phi|^2\right] \cdot \sin\theta \cdot d\theta \cdot d\phi$$

$\not\propto r$

Radiation intensity (power radiated in a given direction per unit solid angle)

$$K = \frac{\eta}{8\lambda^2}\cdot\left[|N_\theta|^2 + |N_\phi|^2\right]$$

$$W = \int_0^\pi \int_0^{2\pi} K \sin\theta \, d\theta \, d\phi$$

(§) Currents in one direction e.g. $\hat{z}$

$\Rightarrow$ $\bar{A}, \bar{N} \sim \hat{z}$

$$N_\phi = 0, \quad N_\theta = -N_z \sin\theta \,, \quad K = \frac{\eta}{8\lambda^2} |N_z|^2 \sin^2\theta$$

(§) Azimuthally Directed currents

$\bar{J}, \bar{A}, \bar{N} \sim \hat{\phi}$

$$K = \frac{\eta}{8\lambda^2} |N_\phi|^2$$

$$W = 2\pi \int_0^\pi K \sin\theta \, d\theta$$

Cartesian $(N_x, N_y, N_z) \longrightarrow$ Spherical coords

$$N_\theta = (N_x \cos\phi + N_y \sin\phi)\cos\theta - N_z \sin\theta$$

$$N_\phi = -N_x \sin\phi + N_y \cos\phi$$

$Q(\theta,\phi)$, $Q'(\theta',\phi')$ $\Rightarrow$ $\cos\Psi = \cos\theta\cos\theta' + \sin\theta\sin\theta'\cos(\phi-\phi')$

Half-wave Dipole

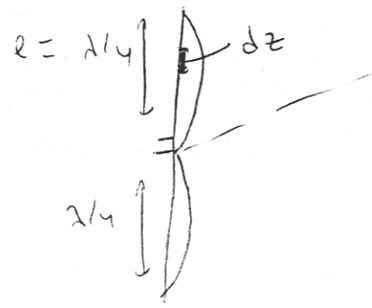

$$\bar{I} = \hat{z}\, I = \hat{z}\begin{cases} I_m \sin[k(\ell - z)], & z \geq 0 \\ I_m \sin[k(\ell + z)], & z < 0 \end{cases}$$

$\Psi = \theta$, $\bar{A}, \bar{N} \sim \hat{z}$

$$\bar{N} = \hat{z}\int_{-\ell}^{\ell} I e^{jkz'\cos\theta}\, dz' =$$

$$= \hat{z}\int_{-\ell}^{0} I_m \sin[k(\ell+z')]\, e^{jkz'\cos\theta}\, dz'$$

$$+ \hat{z}\int_{0}^{\ell} I_m \sin[k(\ell - z')]\, e^{jkz'\cos\theta}\, dz'$$

$$\int e^{ax}\sin(bx+c)\,dx = \frac{e^{ax}}{a^2+b^2}\left[a\sin(bx+c) - b\cos(bx+c)\right]$$

$$\bar{N} = \hat{z}\,\frac{2 I_m}{k\sin^2\theta}\left[\cos(k\ell\cos\theta) - \cos k\ell\right]$$

$N_\theta = -N_z \sin\theta$

$$E_\theta = \frac{j\eta I_m}{2\pi r} e^{-jkr}\left[\frac{\cos(k\ell\cos\theta) - \cos(k\ell)}{\sin\theta}\right], \quad H_\phi = E_\theta/\eta$$

$$K = \frac{\eta I_m^2}{8\pi^2}\left[\frac{\cos(k\ell\cos\theta) - \cos(k\ell)}{\sin\theta}\right]^2, \quad W = \frac{\eta I_m^2}{4\pi}\int_0^\pi \frac{[\cos(k\ell\cos\theta) - \cos(k\ell)]^2}{\sin\theta}\, d\theta$$

Half-wave Dipole: $\ell = \lambda/4$

$$|E_\theta| = \frac{60 I_m}{r}\left[\frac{\cos((\pi/2)\cos\theta)}{\sin\theta}\right] \text{ v/m}, \quad K = \frac{15 I_m^2}{\pi}\left\{\frac{\cos((\pi/2)\cos\theta)}{\sin\theta}\right\}^2 \text{ W/sr}$$

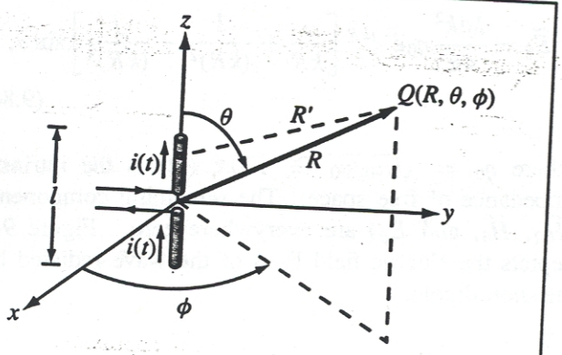

Figure 9-4: Short dipole placed at the origin of a spherical coordinate system.

dipole, which is commonly used as a standard antenna for many applications.

A short dipole, also called a ***Hertzian dipole***, is a thin, linear conductor whose length l is very short compared with the wavelength λ; to satisfy the uniform-current assumption, l should not exceed $\lambda/50$. The wire, which is oriented along the z-direction as shown in Fig. 9-4, carries a sinusoidally varying current given by

$$i(t) = I_0 \cos \omega t = \Re e[I_0 e^{j\omega t}] \quad \text{(A)}, \tag{9.1}$$

where I_0 is the current amplitude. From Eq. (9.1), the phasor current $\tilde{I} = I_0$. Even though the current has to go to zero at the two ends of the dipole, we shall treat it as constant across its entire length.

The customary approach for finding the electric and magnetic fields at a point Q in space [Fig. 9-4] due to radiation by a current source is through the retarded vector potential $\mathbf{A}$. From Eq. (6.84), the phasor retarded vector potential $\tilde{\mathbf{A}}(R)$ at a distance vector $\mathbf{R}$ from a volume v' containing a phasor current distribution $\tilde{\mathbf{J}}$ is given by

$$\tilde{\mathbf{A}}(\mathbf{R}) = \frac{\mu_0}{4\pi} \int_{v'} \frac{\tilde{\mathbf{J}} e^{-jkR'}}{R'} \, dv', \tag{9.2}$$

where μ_0 is the magnetic permeability of free space (because the observation point is in air) and $k = \omega/c = 2\pi/\lambda$ is the wavenumber. For the dipole, the current density is simply $\tilde{\mathbf{J}} = \hat{\mathbf{z}}(I_0/s)$, where s is the cross-sectional area of the dipole wire, $dv' = s\, dz$, and the limits of integration are from $z = -l/2$ to $z = l/2$. In Fig. 9-4, the distance R' between the observation point and a given point along the dipole is not the same as the distance to its center, R, but because we are dealing with a very short dipole, we can set $R' \simeq R$. Hence,

$$\begin{aligned} \tilde{\mathbf{A}} &= \frac{\mu_0}{4\pi} \frac{e^{-jkR}}{R} \int_{-l/2}^{l/2} \hat{\mathbf{z}} I_0 \, dz \\ &= \hat{\mathbf{z}} \frac{\mu_0}{4\pi} I_0 l \left(\frac{e^{-jkR}}{R} \right), \end{aligned} \tag{9.3}$$

The function (e^{-jkR}/R), called the *spherical propagation factor*, accounts for the $1/R$ decay of the magnitude with distance as well as for the phase change represented by e^{-jkR}. The direction of $\tilde{\mathbf{A}}$ is dictated by the direction of flow of the current (z-direction).

Because our objective is to characterize the directional character of the radiated power at a fixed distance R from the antenna, the spherical coordinate system shown in Fig. 9-5 is deemed appropriate for the presentation of antenna pattern plots, with the variables R, θ, and ϕ referred to as the *range*, *zenith angle*, and *azimuth angle*, respectively. To this end, we need to write $\tilde{\mathbf{A}}$ in terms of its spherical coordinate components, which is realized [with the help of Eq. (3.65c)] by expressing $\hat{\mathbf{z}}$ in terms of the unit vectors of the spherical coordinate system:

$$\hat{\mathbf{z}} = \hat{\mathbf{R}} \cos\theta - \hat{\boldsymbol{\theta}} \sin\theta. \tag{9.4}$$

Upon substituting Eq. (9.4) into Eq. (9.3), we have

$$\begin{aligned} \tilde{\mathbf{A}} &= (\hat{\mathbf{R}} \cos\theta - \hat{\boldsymbol{\theta}} \sin\theta) \frac{\mu_0 I_0 l}{4\pi} \left(\frac{e^{-jkR}}{R} \right) \\ &= \hat{\mathbf{R}} \tilde{A}_R + \hat{\boldsymbol{\theta}} \tilde{A}_\theta + \hat{\boldsymbol{\phi}} \tilde{A}_\phi, \end{aligned} \tag{9.5}$$

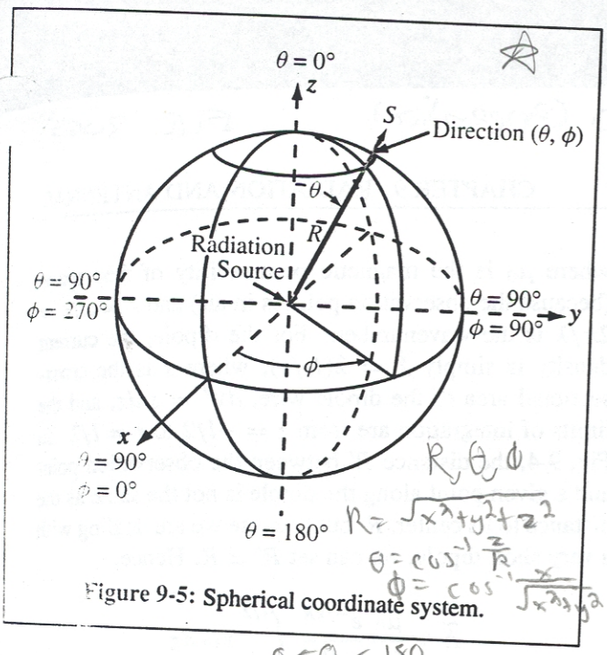

Figure 9-5: Spherical coordinate system.

with

$$\widetilde{A}_R = \frac{\mu_0 I_0 l}{4\pi}\cos\theta\left(\frac{e^{-jkR}}{R}\right), \tag{9.6a}$$

$$\widetilde{A}_\theta = -\frac{\mu_0 I_0 l}{4\pi}\sin\theta\left(\frac{e^{-jkR}}{R}\right), \tag{9.6b}$$

$$\widetilde{A}_\phi = 0.$$

With the spherical coordinate components of $\widetilde{\mathbf{A}}$ known, the next step is straightforward; we simply apply the free-space relationships given by Eqs. (6.85) and (6.86),

$$\widetilde{\mathbf{H}} = \frac{1}{\mu_0}\nabla\times\widetilde{\mathbf{A}}, \tag{9.7a}$$

$$\widetilde{\mathbf{E}} = \frac{1}{j\omega\varepsilon_0}\nabla\times\widetilde{\mathbf{H}}, \tag{9.7b}$$

to obtain the expressions

$$\widetilde{H}_\phi = \frac{I_0 l k^2}{4\pi}e^{-jkR}\left[\frac{j}{kR}+\frac{1}{(kR)^2}\right]\sin\theta \tag{9.8a}$$

$$\widetilde{E}_R = \frac{2I_0 l k^2}{4\pi}\eta_0 e^{-jkR}\left[\frac{1}{(kR)^2}-\frac{j}{(kR)^3}\right]\cos\theta \tag{9.8b}$$

$$\widetilde{E}_\theta = \frac{I_0 l k^2}{4\pi}\eta_0 e^{-jkR}\left[\frac{j}{kR}+\frac{1}{(kR)^2}-\frac{j}{(kR)^3}\right]\sin\theta, \tag{9.8c}$$

where $\eta_0 = \sqrt{\mu_0/\varepsilon_0} \cong 120\pi$ (Ω) is the intrinsic impedance of free space. The remaining components ($\widetilde{H}_R$, $\widetilde{H}_\theta$, and $\widetilde{E}_\phi$) are everywhere zero. Figure 9-6 depicts the electric field lines of the wave radiated by the short dipole.

9-1.1 Far-Field Approximation

As was stated earlier, in most antenna applications, we are primarily interested in the radiation pattern of the antenna at great distances from the source. For the electrical dipole, this corresponds to distances R such that $R \gg \lambda$ or, equivalently, $kR = 2\pi R/\lambda \gg 1$. This condition allows us to neglect the terms varying as $1/(kR)^2$ and $1/(kR)^3$ in Eqs. (9.8a) to (9.8c) in favor of the terms varying as $1/kR$, which yields the far-field expressions

$$\widetilde{E}_\theta = \frac{jI_0 l k\eta_0}{4\pi}\left(\frac{e^{-jkR}}{R}\right)\sin\theta \quad \text{(V/m)}, \tag{9.9a}$$

$$\widetilde{H}_\phi = \frac{\widetilde{E}_\theta}{\eta_0} \quad \text{(A/m)}, \tag{9.9b}$$

and $\widetilde{E}_R$ is negligible. At the observation point Q [Fig. 9-4], the wave now appears to be similar to a uniform plane wave with its electric and magnetic fields in time phase, related by the intrinsic impedance of the medium

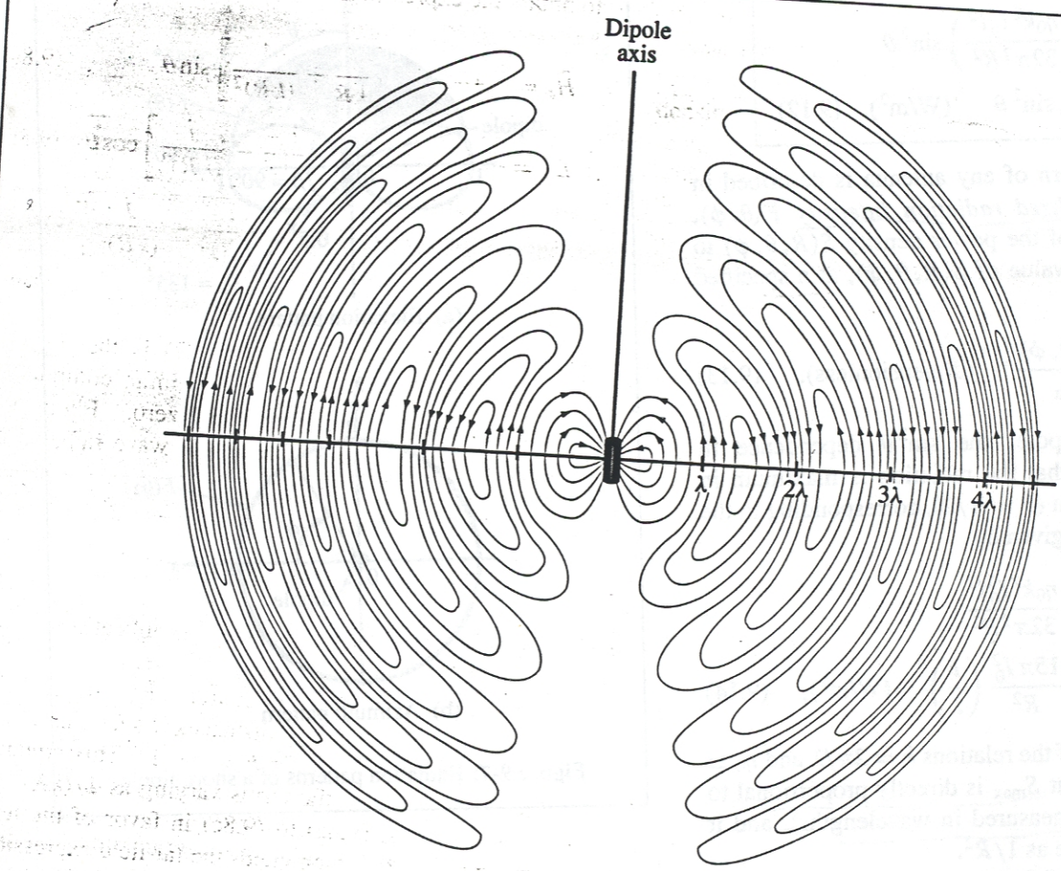

Figure 9-6: Electric field lines surrounding an oscillating dipole at a given instant.

η_0, and orthogonal to each other and to the direction of propagation ($\hat{\mathbf{R}}$). Both fields are proportional to $\sin\theta$ and independent of ϕ (which is as expected from symmetry considerations).

9-1.2 Power Density

Given $\widetilde{\mathbf{E}}$ and $\widetilde{\mathbf{H}}$ in phasor form, the *time-average Poynting vector* of the radiated wave, which is also called the *power density*, can be obtained by applying Eq. (7.101), that is,

$$\mathbf{S}_{av} = \tfrac{1}{2}\mathcal{R}e\left(\widetilde{\mathbf{E}} \times \widetilde{\mathbf{H}}^*\right) \quad (\text{W/m}^2). \tag{9.10}$$

For the short dipole, use of Eqs. (9.9a) and (9.9b) gives

$$\mathbf{S}_{av} = \hat{\mathbf{R}}\, S(R, \theta), \tag{9.11}$$

$$S(R,\theta) = \left(\frac{\eta_0 k^2 I_0^2 l^2}{32\pi^2 R^2}\right)\sin^2\theta$$
$$= S_0 \sin^2\theta \quad (\text{W/m}^2). \quad (9.12)$$

The directional pattern of any antenna is described in terms of the *normalized radiation intensity* $F(\theta,\phi)$, defined as the ratio of the power density $S(R,\theta,\phi)$ to S_{max}, the maximum value of $S(R,\theta,\phi)$, at a specified range R:

$$F(\theta,\phi) = \frac{S(R,\theta,\phi)}{S_{max}} \quad (\text{dimensionless}). \quad (9.13)$$

For the Hertzian dipole, the $\sin^2\theta$ dependence in Eq. (9.12) indicates that the radiation is maximum in the broadside direction ($\theta = \pi/2$), corresponding to the azimuth plane, and is given by

$$S_{max} = S_0 = \frac{\eta_0 k^2 I_0^2 l^2}{32\pi^2 R^2}$$
$$= \frac{15\pi I_0^2}{R^2}\left(\frac{l}{\lambda}\right)^2 \quad (\text{W/m}^2), \quad (9.14)$$

here use was made of the relations $k = 2\pi/\lambda$ and $\eta_0 \simeq 20\pi$. We observe that S_{max} is directly proportional to and to l^2 (with l measured in wavelengths), and it creases with distance as $1/R^2$.

From the definition of the normalized radiation intensity given by Eq. (9.13), it follows that

$$F(\theta,\phi) = F(\theta) = \sin^2\theta. \quad (9.15)$$

ts of $F(\theta)$ are shown in Fig. 9-7 in both the elevation ne (also called the θ-plane) and the azimuth plane plane). No energy is radiated by the dipole along direction of the dipole axis and maximum radiation = 1) occurs in the broadside direction. Since $F(\theta)$ is pendent of ϕ, the pattern is doughnut-shaped in θ–ϕ e.

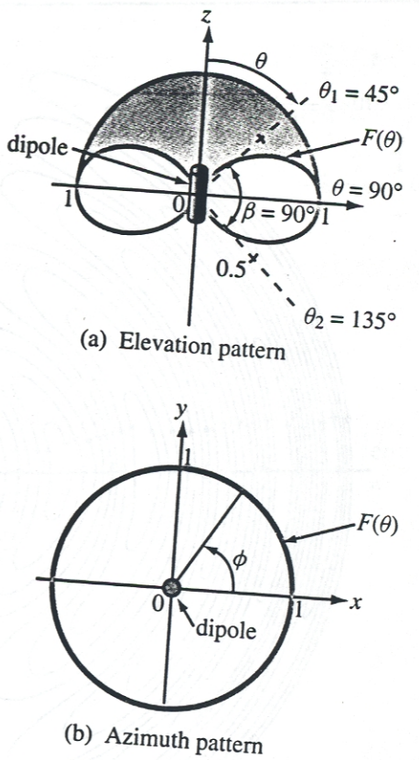

(a) Elevation pattern

(b) Azimuth pattern

Figure 9-7: Radiation patterns of a short dipole.

REVIEW QUESTIONS

Q9.1 When is an antenna a reciprocal device?

Q9.2 What is the radiated wave like in the far-field region of the antenna?

Q9.3 How short should the length of a wire antenna be so that it may be considered a Hertzian dipole? What is the underlying assumption about the current flowing through the wire?

Q9.4 Outline the basic steps used in order to relate the current in the wire to the radiated power density.

EXERCISE 9.1 A 1-m-long dipole is excited by a 5-MHz current with an amplitude of 5 A. At a distance of 2 km, what is the power density radiated by the antenna along its broadside direction?

Ans. $S_0 = 8.2 \times 10^{-8}$ W/m^2.

9-2 Antenna Radiation Characteristics

An *antenna pattern* describes the far-field directional properties of an antenna when measured at a fixed distance from the antenna. In general, the antenna pattern is a three-dimensional plot that displays the strength of the radiated field or power density as a function of direction, with direction being specified by the zenith angle θ and the azimuth angle ϕ. By virtue of the reciprocity theorem, *a receiving antenna has the same directional antenna pattern as the pattern that it exhibits when operated in the transmission mode.*

Consider a transmitting antenna placed at the origin of the observation sphere shown in Fig. 9-8. The differential power radiated by the antenna through an elemental area dA is

$$dP_{\text{rad}} = \mathbf{S}_{\text{av}} \cdot d\mathbf{A} = \mathbf{S}_{\text{av}} \cdot \hat{\mathbf{R}}\, dA = S\, dA \quad \text{(W)}, \tag{9.16}$$

where S is the radial component of the time-average Poynting vector $\mathbf{S}_{\text{av}}$. In the far-field region of any antenna, $\mathbf{S}_{\text{av}}$ is always in the radial direction. In a spherical coordinate system,

$$dA = R^2 \sin\theta\, d\theta\, d\phi, \tag{9.17}$$

and the *solid angle* $d\Omega$ associated with dA, defined as the subtended area divided by R^2, is given by

$$d\Omega = \frac{dA}{R^2} = \sin\theta\, d\theta\, d\phi \quad \text{(sr)}. \tag{9.18}$$

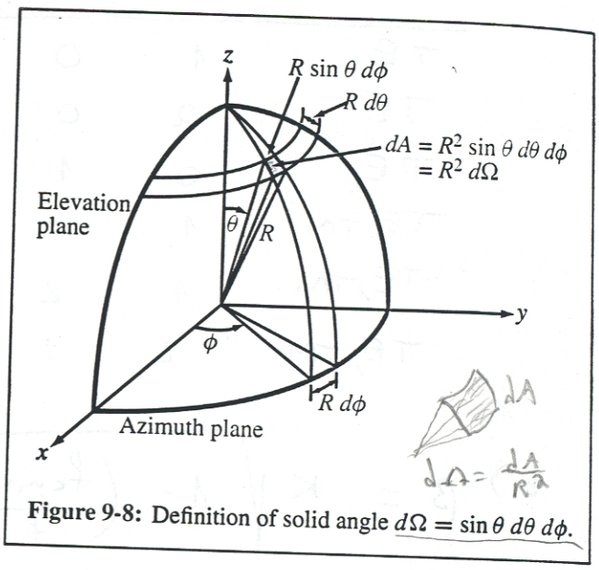

Figure 9-8: Definition of solid angle $d\Omega = \sin\theta\, d\theta\, d\phi$.

Note that, whereas a planar angle is measured in radians and the angular measure of a complete circle is 2π (rad), a solid angle is measured in *steradians* (sr), and the angular measure for a spherical surface is $\Omega = (4\pi R^2)/R^2 = 4\pi$ (sr). The solid angle of a hemisphere is 2π (sr).

Using the relation $dA = R^2\, d\Omega$, dP_{rad} can be rewritten as

$$dP_{\text{rad}} = R^2\, S(R, \theta, \phi)\, d\Omega. \tag{9.19}$$

The total power radiated by an antenna through a spherical surface at a fixed distance R is obtained by integrating Eq. (9.19):

$$\begin{aligned} P_{\text{rad}} &= R^2 \int_{\phi=0}^{2\pi} \int_{\theta=0}^{\pi} S(R, \theta, \phi) \sin\theta\, d\theta\, d\phi \\ &= R^2 S_{\max} \int_{\phi=0}^{2\pi} \int_{\theta=0}^{\pi} F(\theta, \phi) \sin\theta\, d\theta\, d\phi \\ &= R^2 S_{\max} \iint_{4\pi} F(\theta, \phi)\, d\Omega \quad \text{(W)}, \end{aligned} \tag{9.20}$$

Q9.4 Outline the basic steps used in order to relate the current in the wire to the radiated power density.

EXERCISE 9.1 A 1-m-long dipole is excited by a 5-MHz current with an amplitude of 5 A. At a distance of 2 km, what is the power density radiated by the antenna along its broadside direction?

Ans. $S_0 = 8.2 \times 10^{-8}$ W/m^2.

9-2 Antenna Radiation Characteristics

An *antenna pattern* describes the far-field directional properties of an antenna when measured at a fixed distance from the antenna. In general, the antenna pattern is a three-dimensional plot that displays the strength of the radiated field or power density as a function of direction, with direction being specified by the zenith angle θ and the azimuth angle ϕ. By virtue of the reciprocity theorem, *a receiving antenna has the same directional antenna pattern as the pattern that it exhibits when operated in the transmission mode.*

Consider a transmitting antenna placed at the origin of the observation sphere shown in Fig. 9-8. The differential power radiated by the antenna through an elemental area dA is

$$dP_{rad} = \mathbf{S}_{av} \cdot d\mathbf{A} = \mathbf{S}_{av} \cdot \hat{\mathbf{R}}\, dA = S\, dA \quad \text{(W)}, \quad (9.16)$$

where S is the radial component of the time-average Poynting vector $\mathbf{S}_{av}$. In the far-field region of any antenna, $\mathbf{S}_{av}$ is always in the radial direction. In a spherical coordinate system,

$$dA = R^2 \sin\theta\, d\theta\, d\phi, \quad (9.17)$$

and the *solid angle* $d\Omega$ associated with dA, defined as the subtended area divided by R^2, is given by

$$d\Omega = \frac{dA}{R^2} = \sin\theta\, d\theta\, d\phi \quad \text{(sr)}. \quad (9.18)$$

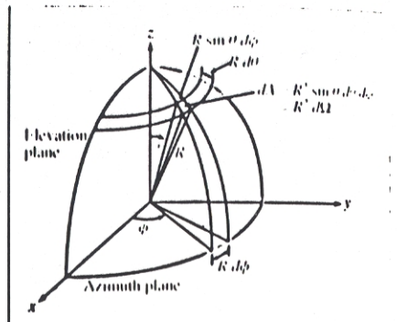

Figure 9-8: Definition of solid angle $d\Omega = \sin\theta\, d\theta\, d\phi$.

Note that, whereas a planar angle is measured in radians and the angular measure of a complete circle is 2π (rad), a solid angle is measured in steradians (sr), and the angular measure for a spherical surface is $\Omega = (4\pi R^2)/R^2 = 4\pi$ (sr). The solid angle of a hemisphere is 2π (sr).

Using the relation $dA = R^2\, d\Omega$, dP_{rad} can be rewritten as

$$dP_{rad} = R^2\, S(R, \theta, \phi)\, d\Omega. \quad (9.19)$$

The total power radiated by an antenna through a spherical surface at a fixed distance R is obtained by integrating Eq. (9.19):

$$\begin{aligned} P_{rad} &= R^2 \int_{\phi=0}^{2\pi} \int_{\theta=0}^{\pi} S(R, \theta, \phi) \sin\theta\, d\theta\, d\phi \\ &= R^2 S_{max} \int_{\phi=0}^{2\pi} \int_{\theta=0}^{\pi} F(\theta, \phi) \sin\theta\, d\theta\, d\phi \\ &= R^2 S_{max} \iint_{4\pi} F(\theta, \phi)\, d\Omega \quad \text{(W)}. \end{aligned} \quad (9.20)$$

where $F(\theta, \phi)$ is the normalized radiation intensity defined by Eq. (9.13). The 4π symbol under the integral sign is used as an abbreviation for the indicated limits on θ and ϕ. Formally, P_{rad} is called the *total radiated power*.

9-2.1 Antenna Pattern

Each specific combination of the zenith angle θ and the azimuth angle ϕ denotes a specific direction in the spherical coordinate system of Fig. 9-8. The normalized radiation intensity $F(\theta, \phi)$ characterizes the directional pattern of the energy radiated by an antenna, and a plot of $F(\theta, \phi)$ as a function of both θ and ϕ constitutes a three-dimensional pattern, an example of which is shown in Fig. 9-9.

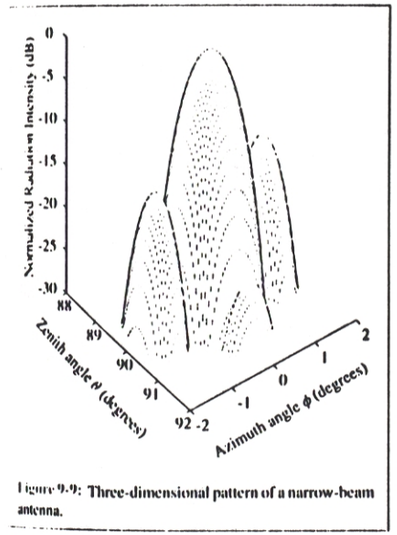

Figure 9-9: Three-dimensional pattern of a narrow-beam antenna.

Often, it is of interest to characterize the variation of $F(\theta, \phi)$ in the form of two-dimensional plots in specific planes in the spherical coordinate system. The two planes most commonly specified for this purpose are the elevation and azimuth planes. The *elevation plane*, also called the θ plane, is the plane corresponding to a constant value of ϕ. For example, $\phi = 0$ defines the x–z plane and $\phi = 90°$ defines the y–z plane, both of which are elevation planes (Fig. 9-8). A plot of $F(\theta, \phi)$ versus θ in either of these planes constitutes a two-dimensional pattern in the elevation plane. This is not to imply, however, that the elevation-plane pattern is necessarily the same in all elevation planes. The *azimuth plane*, also called the ϕ plane, is specified by $\theta = 90°$ and corresponds to the x–y plane. The elevation and azimuth planes are often called the two *principal planes* of the spherical coordinate system.

Some antennas exhibit highly directive patterns with narrow beams, in which case it is found convenient to plot the antenna pattern on a decibel scale by expressing F in decibels:

$$F\,(\text{dB}) = 10 \log F.$$

As an example, the antenna pattern shown in Fig. 9-10(a) is plotted on a decibel scale in polar coordinates, with intensity as the radial variable. This format permits a convenient visual interpretation of the directional distribution of the *radiation lobes*. Another format commonly used for inspecting the pattern of a narrow-beam antenna is the rectangular display shown in Fig. 9-10(b), which permits the pattern to be easily expanded by changing the scale of the horizontal axis. These plots represent the variation in only one plane in the observation sphere, the $\phi = 0$ plane. Unless the pattern is symmetrical in ϕ, additional patterns are required to define the variation of $F(\theta, \phi)$ with θ and ϕ.

Strictly speaking, the polar angle θ is always positive, being defined over the range from 0° (z-direction) to 180° ($-z$-direction), and yet the θ-axis in Fig. 9-10(b) is shown to have both positive and negative values. This

F. T. Ulaby "Fundamentals of Applied EM" Prentice Hall 1999

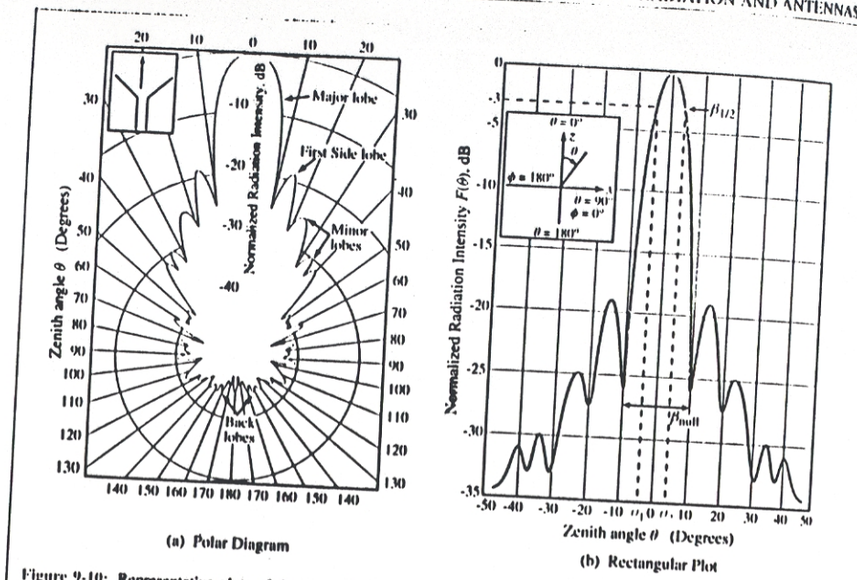

(a) Polar Diagram

(b) Rectangular Plot

Figure 9-10: Representative plots of the normalized radiation pattern of a microwave antenna in (a) polar form and (b) rectangular form.

is not a contradiction, but rather a different form of plotting antenna patterns. The right-hand half of the plot represents the variation of F (dB) with θ as θ is increased in a clockwise direction in the x–z plane [see inset in Fig. 9-10(b)], corresponding to $\phi = 0$, whereas the left-hand half of the plot represents the variation of F (dB) with θ as θ is increased in a counterclockwise direction at $\phi = 180°$. Thus, a negative θ value simply denotes that the direction (θ, ϕ) is in the left-hand half of the x–z plane.

The pattern shown in Fig. 9-10(a) indicates that the antenna is fairly directive, since most of the energy is radiated through a narrow range called the *main lobe*. In addition to the main lobe, the pattern exhibits several *side lobes* and *back lobes* as well. For most applications, these extra lobes are considered undesirable because they represent wasted energy for transmitting antennas and potential interference directions for receiving antennas.

9.2.2 Beam Dimensions

For an antenna with a single main lobe, the *pattern solid angle* Ω_p describes the equivalent width of the main lobe of the antenna pattern [Fig. 9-11]. It is defined as the integral of the normalized radiation intensity $F(\theta, \phi)$ over a sphere:

$$\Omega_p = \iint_{4\pi} F(\theta, \phi)\, d\Omega \quad \text{(sr)}. \tag{9.21}$$

For an isotropic antenna with $F(\theta, \phi) = 1$ in all directions, $\Omega_p = 4\pi$ (sr).

The pattern solid angle characterizes the directional properties of the three-dimensional radiation pattern. To characterize the width of the main lobe in a given plane, the term used is *beamwidth*. The *half-power beamwidth*, or simply the beamwidth β, is defined as the angular width of the main lobe between the two angles at which the magnitude of $F(\theta, \phi)$ is equal to half of its peak value (or -3 dB on a decibel scale). For example, for the pattern displayed in Fig. 9-10(b), β is given by

$$\beta = \theta_2 - \theta_1, \tag{9.22}$$

where θ_1 and θ_2 are the *half-power angles* at which $F(\theta, 0) = 0.5$ (with θ_2 denoting the larger value and θ_1 denoting the smaller one, as shown in the figure). If the pattern is symmetrical and the peak value of $F(\theta, \phi)$ is at $\theta = 0$, then $\beta = 2\theta_2$. For the short-dipole pattern shown earlier in Fig. 9-7(a), $F(\theta)$ is maximum at $\theta = 90°$, θ_2 is at 135°, and θ_1 is at 45°. In this case, $\beta = 135° - 45° = 90°$. The beamwidth β is also known as the *3-dB beamwidth*. In addition to the half-power beamwidth, other beam dimensions may be of interest for certain applications, such as the *null beamwidth* β_{null}, which is the width of the spacing between the first nulls on the two sides of the peak [Fig. 9-10(b)].

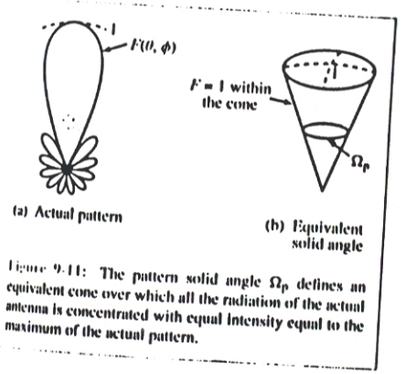

(a) Actual pattern

(b) Equivalent solid angle

Figure 9-11: The pattern solid angle Ω_p defines an equivalent cone over which all the radiation of the actual antenna is concentrated with equal intensity equal to the maximum of the actual pattern.

9-2.3 Antenna Directivity

The *directivity* D of an antenna is defined as the ratio of its maximum normalized radiation intensity, F_{max} (which by definition is equal to 1), to the average value of $F(\theta, \phi)$ over 4π space:

$$D = \frac{F_{max}}{F_{av}} = \frac{1}{\frac{1}{4\pi}\iint_{4\pi} F(\theta, \phi)\, d\Omega} = \frac{4\pi}{\Omega_p} \quad \text{(dimensionless)}. \tag{9.23}$$

where Ω_p is the pattern solid angle defined by Eq. (9.21). Thus, the narrower Ω_p of an antenna pattern is, the greater is the antenna directivity. For an isotropic antenna, $\Omega_p = 4\pi$; hence, its directivity $D_{iso} = 1$.

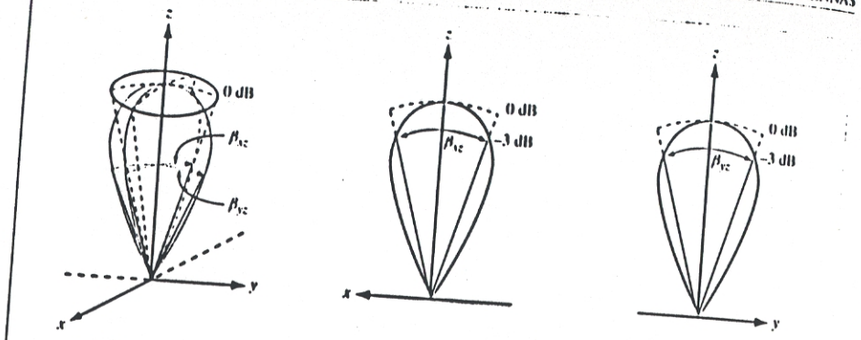

(a) Beam solid angle

(b) Half-power beamwidth in x-z plane

(c) Half-power beamwidth in y-z plane

Figure 9-12: The solid angle of a unidirectional radiation pattern is approximately equal to the product of the half-power beamwidths in the two principal planes; that is, $\Omega_p \simeq \beta_{xz}\beta_{yz}$.

By using Eq. (9.20) in Eq. (9.23), D can be expressed as

$$D = \frac{4\pi R^2 S_{max}}{P_{rad}} = \frac{S_{max}}{S_{av}}, \qquad (9.24)$$

where $S_{av} = P_{rad}/(4\pi R^2)$ is the average value of the radiated power density and is equal to the total power radiated by the antenna, P_{rad}, divided by the surface area of a sphere of radius R. Since $S_{av} = S_{iso}$, where S_{iso} is the power density radiated by an isotropic antenna, D represents the ratio of the maximum power density radiated by the antenna under consideration to the power density radiated by an isotropic antenna, both measured at the same range R and excited by the same amount of input power. Usually, D is expressed in decibels:* D (dB) = 10 log D.

For an antenna with a single main lobe pointing in the z-direction as shown in Fig. 9-12, Ω_p may be approximated as the product of the half-power beamwidths β_{xz} and β_{yz} (in radians):

$$\Omega_p \simeq \beta_{xz}\beta_{yz}, \qquad (9.25)$$

and therefore

$$D = \frac{4\pi}{\Omega_p} \simeq \frac{4\pi}{\beta_{xz}\beta_{yz}}. \qquad (9.26)$$

*A note of caution: even though we often express certain dimensionless quantities in decibels, we should always convert their decibel values to natural values before using them in the relations given in this chapter.

Although approximate, this relation provides a useful method for estimating the antenna directivity from measurements of the beamwidths in the two orthogonal planes whose intersection is the axis of the main lobe.

Example 9-1 Antenna Radiation Properties

Determine (a) the direction of maximum radiation, (b) pattern solid angle, (c) directivity, and (d) half-power beamwidth in the y–z plane for an antenna that radiates into only the upper hemisphere and its normalized radiation intensity is given by $F(\theta, \phi) = \cos^2\theta$.

Solution: Mathematically, the statement that the antenna radiates along directions covering only the upper hemisphere can be written as

$$F(\theta, \phi) = F(\theta) = \begin{cases} \cos^2\theta, & \text{for } 0 \le \theta \le \pi/2 \\ & \text{and } 0 \le \phi \le 2\pi, \\ 0, & \text{elsewhere.} \end{cases}$$

(a) The function $F(\theta) = \cos^2\theta$ is independent of ϕ and is maximum when $\theta = 0°$. A polar plot of $F(\theta)$ is shown in Fig. 9-13.

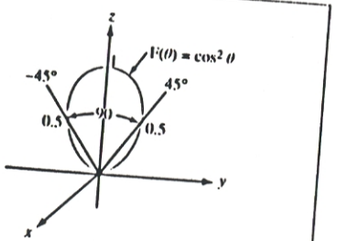

Figure 9-13: Polar plot of $F(\theta) = \cos^2\theta$.

(b) From Eq. (9.21), the pattern solid angle Ω_p is given by

$$\Omega_p = \iint_{4\pi} F(\theta, \phi)\, d\Omega$$
$$= \int_{\phi=0}^{2\pi} \left[\int_{\theta=0}^{\pi/2} \cos^2\theta \sin\theta\, d\theta \right] d\phi$$
$$= \int_{\phi=0}^{2\pi} \left[-\frac{\cos^3\theta}{3} \right]_0^{\pi/2} d\phi$$
$$= \int_0^{2\pi} \frac{1}{3}\, d\phi = \frac{2\pi}{3} \quad \text{(sr)}.$$

(c) Application of Eq. (9.23) gives

$$D = \frac{4\pi}{\Omega_p} = 4\pi \left(\frac{3}{2\pi} \right) = 6,$$

which corresponds to D (dB) = 10 log 6 = 7.78 dB.

(d) The half-power beamwidth β is obtained by setting $F(\theta) = 0.5$. That is,

$$F(\theta) = \cos^2\theta = 0.5,$$

which gives the half-power angles $\theta_1 = -45°$ and $\theta_2 = 45°$. Hence,

$$\beta = \theta_2 - \theta_1 = 90°. \quad \blacksquare$$

Example 9-2 Directivity of a Hertzian Dipole

Calculate the directivity of a Hertzian dipole.

Solution: Application of Eq. (9.23) with $F(\theta) = \sin^2\theta$ [from Eq. (9.15)] gives

$$D = \frac{4\pi}{\iint_{4\pi} F(\theta, \phi) \sin\theta\, d\theta\, d\phi}$$
$$= \frac{4\pi}{\int_{\phi=0}^{2\pi} \int_{\theta=0}^{\pi} \sin^3\theta\, d\theta\, d\phi} = \frac{4\pi}{8\pi/3} = 1.5$$

or, equivalently, 1.76 dB. $\blacksquare$

9-2.4 Antenna Gain

Of the total power P_t (transmitter power) supplied to the antenna, a part, P_{rad}, is radiated out into space, and the remainder, P_{loss}, is dissipated as heat loss in the antenna structure. The *radiation efficiency* ξ is defined as the ratio of P_{rad} to P_t:

$$\xi = \frac{P_{rad}}{P_t} \quad \text{(dimensionless)}. \tag{9.27}$$

The *gain* of an antenna is defined as

$$G = \frac{4\pi R^2 S_{max}}{P_t}, \tag{9.28}$$

which is similar in form to the expression given by Eq. (9.24) for the directivity D except that it is referred to the input power supplied to the antenna, P_t, rather than to the radiated power P_{rad}. In view of Eq. (9.27),

$$G = \xi D \quad \text{(dimensionless)}. \tag{9.29}$$

The gain accounts for ohmic losses in the antenna material, whereas the directivity does not. For a lossless antenna, $\xi = 1$.

9-2.5 Radiation Resistance

To the transmission line connected to its terminal, an antenna is merely an impedance. If the transmission line is matched to the antenna impedance, part of P_t, the power supplied by the generator, is radiated out into space, and the remainder is dissipated as heat in the antenna. The resistance part of the antenna impedance may be defined as consisting of a *radiation resistance* R_{rad} and a *loss resistance* R_{loss}. The corresponding time-average radiated power P_{rad} and dissipated power P_{loss} are

$$P_{rad} = \frac{1}{2} I_0^2 R_{rad}, \tag{9.30a}$$

$$P_{loss} = \frac{1}{2} I_0^2 R_{loss}, \tag{9.30b}$$

where I_0 is the amplitude of the sinusoidal current exciting the antenna. As defined earlier, the radiation efficiency is the ratio of P_{rad} to P_t,

$$\xi = \frac{P_{rad}}{P_t} = \frac{P_{rad}}{P_{rad} + P_{loss}} = \frac{R_{rad}}{R_{rad} + R_{loss}}. \tag{9.31}$$

The radiation resistance R_{rad} can be calculated by integrating the far-field power density over a sphere to obtain P_{rad} and then equating the result to Eq. (9.30a).

Example 9-3 Radiation Resistance and Efficiency of a Hertzian Dipole

A 4-cm-long center-fed dipole is used as an antenna at 75 MHz. The antenna wire is made of copper and has a radius $a = 0.4$ mm. From Eqs. (7.92a) and (7.94), the loss resistance of a circular wire of length l is given by

$$R_{loss} = \frac{l}{2\pi a}\sqrt{\frac{\pi f \mu_c}{\sigma_c}}, \tag{9.32}$$

where μ_c and σ_c are the magnetic permeability and conductivity of the wire, respectively. Calculate the radiation resistance and the radiation efficiency of the dipole antenna.

Solution: At 75 MHz,

$$\lambda = \frac{c}{f} = \frac{3 \times 10^8}{7.5 \times 10^7} = 4 \text{ m}.$$

The length to wavelength ratio is $l/\lambda = 4$ cm/4 m $= 10^{-2}$. Hence, this is a short dipole. From Eq. (9.24), P_{rad} is given by

$$P_{rad} = \frac{4\pi R^2}{D} S_{max}. \tag{9.33}$$

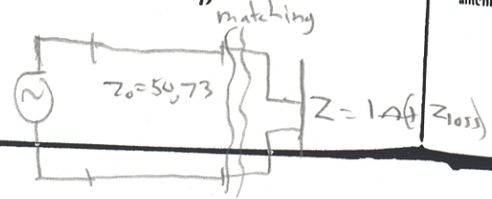

For the Hertzian dipole, S_{max} is given by Eq. (9.14), and from Example 9-2 we established that $D = 1.5$. Hence,

$$P_{rad} = \frac{4\pi R^2}{1.5} \times \frac{15\pi I_0^2}{R^2}\left(\frac{l}{\lambda}\right)^2 = 40\pi^2 I_0^2 \left(\frac{l}{\lambda}\right)^2. \tag{9.34}$$

Equating this result to Eq. (9.30a) and then solving for the radiation resistance R_{rad} gives

$$R_{rad} = 80\pi^2 (l/\lambda)^2 \quad (\Omega). \tag{9.35}$$

For $l/\lambda = 10^{-2}$, $R_{rad} = 0.08\ \Omega$.

Next, we will find the loss resistance R_{loss}. For copper, Appendix B gives $\mu_c \simeq \mu_0 = 4\pi \times 10^{-7}$ H/m and $\sigma_c = 5.8 \times 10^7$ S/m. Hence,

$$R_{loss} = \frac{l}{2\pi a}\sqrt{\frac{\pi f \mu_c}{\sigma_c}} = \frac{4 \times 10^{-2}}{2\pi \times 4 \times 10^{-4}}\left[\frac{\pi \times 75 \times 10^6 \times 4\pi \times 10^{-7}}{5.8 \times 10^7}\right]^{1/2} = 0.036\ \Omega,$$

and therefore the radiation efficiency is

$$\xi = \frac{R_{rad}}{R_{rad} + R_{loss}} = \frac{0.08}{0.08 + 0.036} = 0.69,$$

or 69% efficient. ■

REVIEW QUESTIONS

Q9.5 What does the pattern solid angle represent?

Q9.6 What is the magnitude of the directivity of an isotropic antenna?

Q9.7 What physical and material properties affect the radiation efficiency of a fixed-length Hertzian dipole antenna?

EXERCISE 9.2 An antenna has a conical radiation pattern with a normalized radiation intensity $F(\theta) = 1$ for θ between 0° and 45° and zero intensity for θ between 45° and 180°. The pattern is independent of the azimuth angle ϕ. Find (a) the pattern solid angle and (b) the directivity.

Ans. (a) $\Omega_p = 1.84$ sr, (b) $D = 6.83$ or, equivalently, 8.3 dB.

EXERCISE 9.3 The maximum power density radiated by a short dipole at a distance of 1 km is 60 (nW/m^2). If $I_0 = 10$ A, find the radiation resistance.

Ans. $R_{rad} = 10\ \text{m}\Omega$.

9-3 Half-Wave Dipole Antenna

In Section 9-1 we developed expressions for the electric and magnetic fields radiated by a short dipole of length much shorter than λ. We shall now use these expressions as building blocks to obtain expressions for the fields radiated by a half-wave dipole antenna, so named because its length $l = \lambda/2$. As shown in Fig. 9-14, the half-wave dipole consists of a thin wire fed at its center by a generator connected to the antenna terminals via a transmission line. The current flowing through the wire has a symmetrical distribution with respect to the center of the dipole, and the current has to be zero at the ends. Mathematically, $i(t)$ is given by

$$i(t) = I_0 \cos\omega t \cos kz = \Re e\left[I_0 \cos kz\, e^{j\omega t}\right], \tag{9.36}$$

whose current phasor is

$$\tilde{I}(z) = I_0 \cos kz, \qquad \frac{-\lambda}{4} \le z \le \frac{\lambda}{4}, \tag{9.37}$$

and $k = 2\pi/\lambda$. Equation (9.9a) gives an expression for $\tilde{E}_\theta$, the far field (at distance R) radiated by a short dipole of length l when excited by a current I_0. Let us adapt that expression to an infinitesimal dipole segment

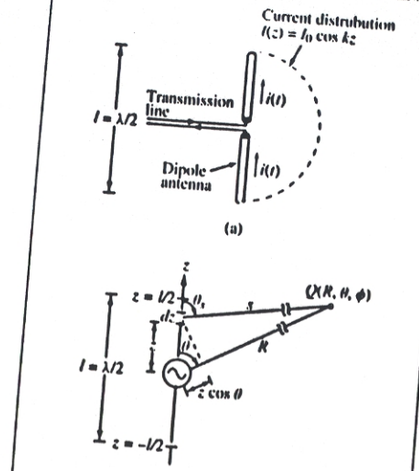

Figure 9-14: Center-fed half-wave dipole.

of length dz, excited by a current $\tilde{I}(z)$ and located at a distance s from the observation point [Fig. 9-14(b)]. Thus,

$$d\tilde{E}_\theta(z) = \frac{jk\eta_0}{4\pi}\tilde{I}(z)\,dz\left(\frac{e^{-jks}}{s}\right)\sin\theta_z, \quad (9.38a)$$

and the associated magnetic field is

$$d\tilde{H}_\phi(z) = \frac{d\tilde{E}_\theta(z)}{\eta_0}. \quad (9.38b)$$

The far field due to radiation by the entire antenna is obtained by integrating the fields from all the Hertzian dipoles making up the antenna:

$$\tilde{E}_\theta = \int_{z=-\lambda/4}^{\lambda/4} d\tilde{E}_\theta. \quad (9.39)$$

Before we calculate this integral, we shall make the following two approximations. The first approximation relates to the magnitude part of the spherical propagation factor, $1/s$. In Fig. 9-14(b), the distance s between the current element and the observation point Q is considered so large in comparison to the length of the dipole that the difference between s and R may be neglected in terms of its effect on $1/s$. Hence, we may set $1/s \simeq 1/R$, and by the same argument we set $\theta_z \simeq \theta$. The error Δ between s and R is a maximum when the observation point is along the z-axis and it is equal to $\lambda/4$ (corresponding to half of the antenna length). If $R \gg \lambda$, this error will have an insignificant effect on $1/s$. For the phase factor e^{-jks}, such an error in distance corresponds to an error in phase of $k\Delta = (2\pi/\lambda)(\lambda/4) = \pi/2$. As a rule of thumb, a phase error greater than $\pi/8$ is considered unacceptable because it may lead to a significant error in the computed value of the field $\tilde{E}_\theta$. Hence, the approximation $s \simeq R$ is too crude for the phase factor and cannot be used. A more tolerable option is to use the parallel-ray approximation given by

$$s \simeq R - z\cos\theta, \quad (9.40)$$

as illustrated in Fig. 9-14(b).

Substituting Eq. (9.40) for s in the phase factor of Eq. (9.38a) and replacing s with R and θ_z with θ elsewhere in the expression, we have

$$d\tilde{E}_\theta = \frac{jk\eta_0}{4\pi}\tilde{I}(z)\,dz\left(\frac{e^{-jkR}}{R}\right)\sin\theta\, e^{jkz\cos\theta}. \quad (9.41)$$

After (1) inserting Eq. (9.41) into Eq. (9.39), (2) using the expression for $\tilde{I}(z)$ given by Eq. (9.37), and (3)

carrying out the integration, the following expressions are obtained:

$$\tilde{E}_\theta = j60I_0\left[\frac{\cos[(\pi/2)\cos\theta]}{\sin\theta}\right]\left(\frac{e^{-jkR}}{R}\right), \quad (9.42a)$$

$$\tilde{H}_\phi = \frac{\tilde{E}_\theta}{\eta_0}. \quad (9.42b)$$

and the corresponding time-average power density is

$$S(R,\theta) = \frac{|\tilde{E}_\theta|^2}{2\eta_0} = \frac{15I_0^2}{\pi R^2}\left[\frac{\cos^2[(\pi/2)\cos\theta]}{\sin^2\theta}\right] = S_0\left[\frac{\cos^2[(\pi/2)\cos\theta]}{\sin^2\theta}\right] \quad (W/m^2). \quad (9.43)$$

Examination of Eq. (9.43) reveals that $S(R,\theta)$ is maximum at $\theta = \pi/2$, and its value is

$$S_{max} = S_0 = \frac{15I_0^2}{(\pi R^2)}.$$

Hence, the normalized radiation intensity is

$$F(\theta) = \frac{S(R,\theta)}{S_0} = \left[\frac{\cos[(\pi/2)\cos\theta]}{\sin\theta}\right]^2. \quad (9.44)$$

The radiation pattern of the half-wave dipole exhibits roughly the same doughnutlike shape shown earlier in Fig. 9-7 for the short dipole. Its directivity is slightly larger (1.64 compared to 1.5 for the short dipole), but its radiation resistance is 73 Ω (as will be shown later in Section 9-3.2), which is orders of magnitude larger than that of a short dipole.

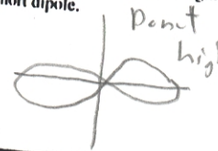

9-3.1 Directivity of $\lambda/2$ Dipole

To evaluate both the directivity D and the radiation resistance R_{rad} of the half-wave dipole, we first need to calculate the total radiated power P_{rad} by applying Eq. (9.20):

$$P_{rad} = R^2\iint_{4\pi} S(R,\theta)\,d\Omega = \frac{15I_0^2}{\pi}\int_0^{2\pi}\int_0^{\pi}\left[\frac{\cos[(\pi/2)\cos\theta]}{\sin\theta}\right]^2\sin\theta\,d\theta\,d\phi. \quad (9.45)$$

The integration over ϕ is equal to 2π, and numerical evaluation of the integration over θ gives the value 1.22. Consequently,

$$P_{rad} = 36.6\,I_0^2 \quad (W). \quad (9.46)$$

From Eq. (9.43), we found that $S_{max} = 15I_0^2/(\pi R^2)$. Using this in Eq. (9.24) gives the following result for the directivity D of the half-wave dipole:

$$D = \frac{4\pi R^2 S_{max}}{P_{rad}} = \frac{4\pi R^2}{36.6I_0^2}\left(\frac{15I_0^2}{\pi R^2}\right) = 1.64 \quad (9.47)$$

or, equivalently, 2.15 dB.

9-3.2 Radiation Resistance of $\lambda/2$ Dipole

Using Eq. (9.30a) to relate the radiation resistance R_{rad} to the total radiated power P_{rad}, we have

$$R_{rad} = \frac{2P_{rad}}{I_0^2} = \frac{2\times 36.6I_0^2}{I_0^2} \simeq 73\ \Omega. \quad (9.48)$$

As was noted earlier in Example 9-3, because the radiation resistance of a short dipole is comparable in magnitude to that of its loss resistance R_{loss}, its radiation efficiency ξ is quite small. For the 4-cm-long dipole of Example 9-3, $R_{rad} = 0.08\ \Omega$ (at 75 MHz) and $R_{loss} = 0.036\ \Omega$. If we keep the frequency the same and increase the length of the dipole to 2 m ($\lambda = 4$ m

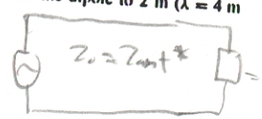

at $f = 75$ MHz), R_{rad} becomes 73 Ω and R_{loss} increases to 1.8 Ω. The radiation efficiency increases from 69% for the short dipole to 98% for the half-wave dipole. More significant is the fact that it is practically impossible to match a transmission line to an antenna with a resistance on the order of 0.1 Ω, while it is quite easy to do so when $R_{rad} = 73$ Ω.

Another interesting feature of the half-wave dipole pertains to its reactance. As seen by a transmission line, an antenna may be represented by an *input impedance* connected to the line at the antenna terminals. The input impedance Z_{in} consists of a real part R_{in} and an imaginary part X_{in}:

$$Z_{in} = R_{in} + jX_{in}. \tag{9.49}$$

where R_{in} is the sum of the radiation resistance R_{rad} and the loss resistance R_{loss},

$$R_{in} = R_{rad} + R_{loss}. \tag{9.50}$$

For the half-wave dipole, R_{loss} is much smaller than R_{rad} and can be ignored. Hence,

$$Z_{in} \cong R_{rad} + jX_{in}. \tag{9.51}$$

Deriving an expression for X_{in} for the half-wave dipole is fairly complicated and beyond the scope of this book. However, it is significant to note that X_{in} is a strong function of l/λ, and it decreases from 42 Ω at $l/\lambda = 0.5$ down to zero at $l/\lambda = 0.48$, whereas R_{rad} remains approximately unchanged. Hence, by reducing the length of the half-wave dipole by 4%, Z_{in} becomes purely real and equal to 73 Ω, thereby making it possible to match the dipole to a 75-Ω transmission line without resorting to the use of a matching network.

9-3.3 Quarter-Wave Monopole Antenna

When placed over a conducting ground plane, a quarter-wave monopole antenna excited by a source at its base [Fig. 9-15(a)] exhibits the same radiation pattern in the region above the ground plane as a half-wave dipole in free space. This is because, from image theory [Section 4-12], the conducting plane can be replaced with the image of the λ/4 monopole, as illustrated in Fig. 9-15(b). Thus, the λ/4 monopole will radiate an electric field identical to that given by Eq. (9.42a), and its normalized radiation intensity is given by Eq. (9.44):

Image Theory principle

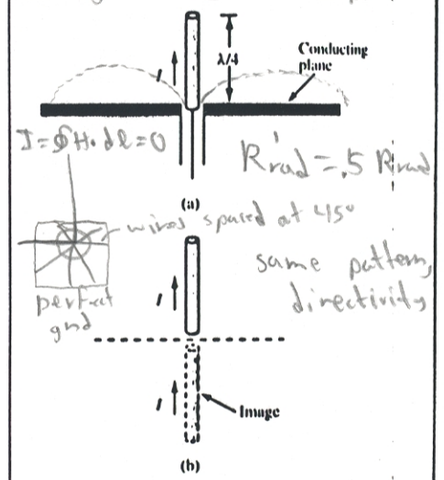

Figure 9-15: A quarter-wave monopole above a conducting plane is equivalent to a full half-wave dipole in free space.

but the radiation is limited to the upper half-space defined by $0 \le \theta \le \pi/2$. Hence, a monopole radiates only half as much power as the dipole. Consequently, for a λ/4 monopole, $P_{rad} = 18.3I_0^2$ and its radiation resistance is $R_{rad} = 36.5$ Ω.

The approach used for the quarter-wave monopole is also valid for any vertical wire antenna placed above a conducting plane, including a Hertzian monopole.

REVIEW QUESTIONS

Q9.8 What is the physical length of a half-wave dipole operating at (a) 1 MHz (in the AM broadcast band), (b) 100 MHz (FM broadcast band), and (c) 10 GHz (microwave band)?

Q9.9 How does the radiation pattern of a half-wave dipole compare with that of a Hertzian dipole? How do their directivities, radiation resistances, and radiation efficiencies compare?

Q9.10 How does the radiation efficiency of a quarter-wave monopole compare with that of a half-wave dipole, assuming that both are made of the same material and have the same cross section?

EXERCISE 9.4 For the half-wave dipole antenna, evaluate $F(\theta)$ versus θ in order to determine the half-power beamwidth in the elevation plane (the plane containing the dipole axis).

Ans. $\beta = 78°$.

EXERCISE 9.5 If the maximum power density radiated by a half-wave dipole is 50 (μW/m^2) at a range of 1 km, what is the current amplitude I_0?

Ans. $I_0 = 3.24$ A.

9-4 Dipole of Arbitrary Length

So far, we have examined the radiation properties of the short Hertzian dipole and of the half-wave dipole. We will now consider the more general case of a linear dipole of any arbitrary length l, relative to λ. For a center-fed dipole, as depicted in Fig. 9-16, the currents flowing through its two halves are symmetrical and must go to zero at its ends. Hence, the current phasor $\tilde{I}(z)$ can be expressed as a sine function with an argument that goes to zero at $z = \pm l/2$:

$$\tilde{I}(z) = \begin{cases} I_0 \sin[k(l/2 - z)], & \text{for } 0 \le z \le l/2, \\ I_0 \sin[k(l/2 + z)], & \text{for } -l/2 \le z < 0, \end{cases} \tag{9.52}$$

where I_0 is the current amplitude. The procedure for calculating the electric and magnetic fields and the

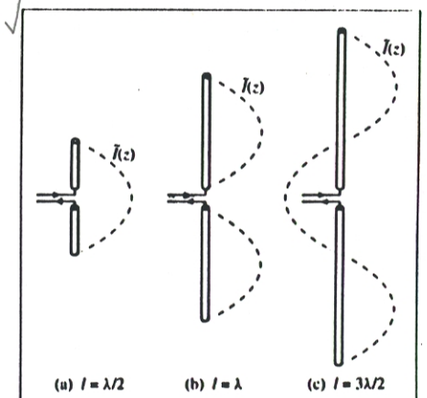

Figure 9-16: Current distribution for three center-fed dipoles.

larger l → higher D

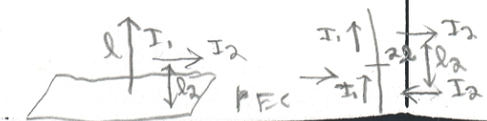

normal to surface - even symmetry almost
|| to surface - odd symmetry - no radiation
more metal loss w/ metal plate

associated power density of the wave radiated by such an antenna is basically the same as that used previously in connection with the half-wave dipole antenna. The only difference is the current distribution $\tilde{I}(z)$. If we insert the expression for $\tilde{I}(z)$ given by Eq. (9.52) in Eq. (9.41), we obtain the following expression for the differential electric field $d\tilde{E}_\theta$ of the wave radiated by an elemental length dz at location z along the dipole:

$$d\tilde{E}_\theta = \frac{jk\eta_0 I_0}{4\pi}\left(\frac{e^{-jkR}}{R}\right)\sin\theta\, e^{jkz\cos\theta}\, dz \times \begin{cases} \sin[k(l/2 - z)], & \text{for } 0 \le z \le l/2, \\ \sin[k(l/2 + z)], & \text{for } -l/2 \le z < 0. \end{cases} \tag{9.53}$$

The total field radiated by the dipole is

$$\begin{aligned} \tilde{E}_\theta &= \int_{-l/2}^{l/2} d\tilde{E}_\theta \\ &= \int_0^{l/2} d\tilde{E}_\theta + \int_{-l/2}^{0} d\tilde{E}_\theta \\ &= \frac{jk\eta_0 I_0}{4\pi}\left(\frac{e^{-jkR}}{R}\right)\sin\theta \\ &\quad \times \left[\int_0^{l/2} e^{jkz\cos\theta}\sin[k(l/2 - z)]\, dz \right. \\ &\quad \left. + \int_{-l/2}^{0} e^{jkz\cos\theta}\sin[k(l/2 + z)]\, dz\right]. \end{aligned} \tag{9.54}$$

If we apply Euler's identity to express $e^{jkz\cos\theta}$ as $[\cos(kz\cos\theta) + j\sin(kz\cos\theta)]$, we can integrate the two integrals and obtain the result

$$\tilde{E}_\theta = j60 I_0\left(\frac{e^{-jkR}}{R}\right) \times \left[\frac{\cos\left(\frac{kl}{2}\cos\theta\right) - \cos\left(\frac{kl}{2}\right)}{\sin\theta}\right]. \tag{9.55}$$

The corresponding time-average power density radiated by the dipole antenna is given by

$$S(\theta) = \frac{|\tilde{E}_\theta|^2}{2\eta_0} = \frac{15 I_0^2}{\pi R^2}\left[\frac{\cos\left(\frac{\pi l}{\lambda}\cos\theta\right) - \cos\left(\frac{\pi l}{\lambda}\right)}{\sin\theta}\right]^2, \tag{9.56}$$

where we have used the relations $\eta_0 \simeq 120\pi\ (\Omega)$ and $k = 2\pi/\lambda$. For $l = \lambda/2$, Eq. (9.56) reduces to the expression given by Eq. (9.43) for the half-wave dipole. Plots of the normalized radiation intensity, $F(\theta) = S(R, \theta)/S_{max}$, are shown in Fig. 9-17 for dipoles with lengths of $\lambda/2$, λ, and $3\lambda/2$. The dipoles with $l = \lambda/2$ and $l = \lambda$ have similar radiation patterns with maxima along $\theta = 90°$, but the half-power beamwidth of the wavelength-long dipole is narrower than that of the half-wave dipole, and $S_{max} = 60 I_0^2/(\pi R^2)$ for the wavelength-long dipole, which is four times that for the half-wave dipole. The pattern of the dipole with length $l = 3\lambda/2$ exhibits a multiple lobe structure, and its direction of maximum radiation is not along $\theta = 90°$.

9-5 Effective Area of a Receiving Antenna

So far, we have examined the radiation characteristics of antennas by treating them as radiators of the energy supplied by a source. Now we shall consider the reverse process, that is, how a receiving antenna extracts energy from an incident wave and delivers it to a load. The ability of an antenna to capture energy from an incident wave of power density S_i (W/m^2) and to convert it into an *intercepted power* P_{int} (W) for delivery to a matched load is characterized by the *effective area* A_e:

$$A_e = \frac{P_{int}}{S_i}\ (\text{m}^2). \tag{9.57}$$

Other commonly used names for A_e include *effective aperture* and *receiving cross section*. The antenna

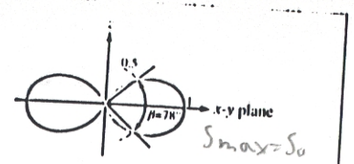

(a) $l = \lambda/2$

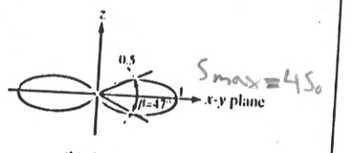

(b) $l = \lambda$

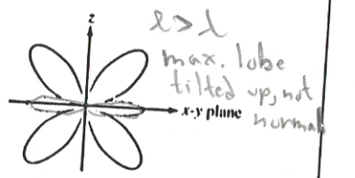

(c) $l = 3\lambda/2$

Figure 9-17: Radiation patterns of dipoles with lengths of $\lambda/2$, λ, and $3\lambda/2$.

receiving process may be modeled in the form of a Thévenin equivalent circuit as shown in Fig. 9-18, where $\tilde{V}_{oc}$ is the open-circuit voltage phasor induced in the receiving antenna by the incident wave, Z_{in} is the antenna impedance, and Z_L is the impedance of the load for which the received power is intended. In general, both Z_{in} and

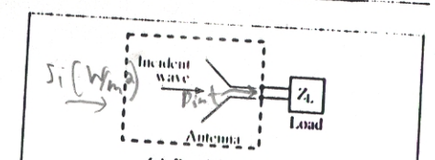

(a) Receiving antenna

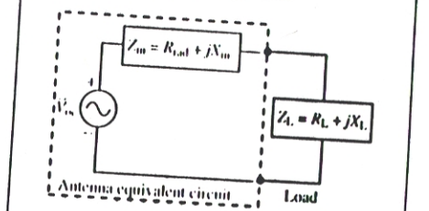

(b) Equivalent circuit

Figure 9-18: Receiving antenna represented by an equivalent circuit.

Z_L are complex:

$$Z_{in} = R_{rad} + jX_{in}, \tag{9.58a}$$

$$Z_L = R_L + jX_L, \tag{9.58b}$$

where R_{rad} denotes the radiation resistance of the antenna, and it is assumed that the antenna loss resistance is much smaller than R_{rad} and can be ignored. As we will see later in Example 9-4, for maximum power transfer, the load impedance must be chosen such that $Z_L = Z_{in}^*$, or $R_L = R_{rad}$ and $X_L = -X_{in}$, in which case the circuit reduces to a source $\tilde{V}_{oc}$ connected across a resistance equal to $2R_{rad}$. Since $\tilde{V}_{oc}$ is a sinusoidal voltage phasor, the time-average power delivered to the load is

$$P_L = \frac{1}{2}|\tilde{I}_L|^2 R_{rad} = \frac{1}{2}\left[\frac{|\tilde{V}_{oc}|}{2R_{rad}}\right]^2 R_{rad} = \frac{|\tilde{V}_{oc}|^2}{8R_{rad}}. \tag{9.59}$$

where $\tilde{I}_L = \tilde{V}_{oc}/(2R_{rad})$ is the phasor current flowing through the circuit. Since the antenna is lossless, all the intercepted power P_{int} ends up in the load resistance R_L. Hence,

$$P_{int} = P_L = \frac{|\tilde{V}_{oc}|^2}{8R_{rad}}. \quad (9.60)$$

For an incident wave with electric field $\tilde{E}_i$ parallel to the antenna polarization direction, the power density carried by the wave is

$$S_i = \frac{|\tilde{E}_i|^2}{2\eta_0} = \frac{|\tilde{E}_i|^2}{240\pi}. \quad (9.61)$$

The ratio of the results provided by Eqs. (9.60) and (9.61) gives

$$A_e = \frac{P_{int}}{S_i} = \frac{30\pi|\tilde{V}_{oc}|^2}{R_{rad}|\tilde{E}_i|^2}. \quad (9.62)$$

The open-circuit voltage $\tilde{V}_{oc}$ induced in the receiving antenna is due to the incident field $\tilde{E}_i$, but the relation between them depends on the specific antenna under consideration. By way of illustration, let us consider the case of the short-dipole antenna of Section 9-1. Because the length l of the short dipole is small compared to λ, the current induced by the incident field will be uniform across its length, and the open-circuit voltage will simply be $\tilde{V}_{oc} = \tilde{E}_i l$. Noting that $R_{rad} = 80\pi^2(l/\lambda)^2$ for the short dipole [see Eq. (9.35)] and using $\tilde{V}_{oc} = \tilde{E}_i l$, Eq. (9.62) simplifies to

$$\boxed{A_e = \frac{3\lambda^2}{8\pi} \quad (\text{m}^2) \quad \text{(short dipole).}} \quad (9.63)$$

In Example 9-2 it was shown that for the short dipole the directivity $D = 1.5$. In terms of D, Eq. (9.63) can be rewritten in the form

$$\boxed{A_e = \frac{\lambda^2 D}{4\pi} \quad (\text{m}^2) \quad \text{(any antenna).}} \quad (9.64)$$

larger than physical area

Despite the fact that the relation between A_e and D given by Eq. (9.64) was derived for a short dipole, it can be shown that it is also valid *for any antenna* under matched impedance conditions.

Example 9-4 Maximum Power Transfer

The circuit shown in Fig. 9-18(b) consists of a generator comprised of a voltage phasor $\tilde{V}_{oc}$ and an internal impedance Z_{in} connected to a load Z_L. If

$$\boxed{\begin{aligned} Z_{in} &= R_{rad} + jX_{in}, \\ Z_L &= R_L + jX_L, \end{aligned}}$$

what values of R_L and X_L yield the maximum transfer of power from the generator into the load?

Solution: The current phasor flowing through the circuit is

$$\tilde{I}_L = \frac{\tilde{V}_{oc}}{Z_{in} + Z_L} = \frac{\tilde{V}_{oc}}{(R_{rad} + R_L) + j(X_{in} + X_L)}, \quad (9.65)$$

and the time-average power dissipated in the load resistance R_L is

$$P_L = \tfrac{1}{2}|\tilde{I}_L|^2 R_L = \tfrac{1}{2}|\tilde{V}_{oc}|^2 \frac{R_L}{(R_{rad} + R_L)^2 + (X_{in} + X_L)^2}. \quad (9.66)$$

Our task is to specify the load parameters, R_L and X_L, that maximize P_L. This is achieved by differentiating the expression for P_L with respect to R_L, equating it to zero, and then repeating the process with respect to X_L. The first of these two steps gives

$$\frac{\partial P_L}{\partial R_L} = \tfrac{1}{2}|\tilde{V}_{oc}|^2 \left[\frac{1}{(R_{rad} + R_L)^2 + (X_{in} + X_L)^2} + \frac{-2R_L(R_{rad} + R_L)}{[(R_{rad} + R_L)^2 + (X_{in} + X_L)^2]^2}\right] = 0,$$

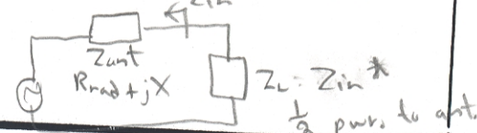

½ pwr. to ant, ½ to load

which yields the result

$$(X_{in} + X_L)^2 - R_L^2 + R_{rad}^2 = 0. \quad (9.67)$$

Application of the second step gives

$$\frac{\partial P_L}{\partial X_L} = \tfrac{1}{2}|\tilde{V}_{oc}|^2 \left[\frac{-2R_L(X_{in} + X_L)}{[(R_{rad} + R_L)^2 + (X_{in} + X_L)^2]^2}\right] = 0,$$

which yields a second condition,

$$R_L(X_{in} + X_L) = 0. \quad (9.68)$$

To satisfy this result, we have to choose either $R_L = 0$, which is not an acceptable result because it means that $P_L = 0$, or

$$\boxed{X_L = -X_{in}.} \quad (9.69a)$$

Using Eq. (9.69a) in Eq. (9.67) gives

$$\boxed{R_L = R_{rad}.} \quad (9.69b)$$

These two results can be combined into

$$\boxed{Z_L = Z_{in}^*.} \quad (9.70)$$

where Z_{in}^* is the complex conjugate of Z_{in}. Thus, *for maximum power transfer, the load impedance should be equal to the complex conjugate of the generator impedance.* ■

EXERCISE 9.6 The effective area of an antenna is 9 m². What is its directivity in decibels at 3 GHz?

Ans. $D = 40.53$ dB.

EXERCISE 9.7 At 100 MHz, the pattern solid angle of an antenna is 1.3 sr. Find (a) the antenna directivity D and (b) its effective area A_e.

Ans. (a) $D = 9.67$, (b) $A_e = 6.92$ m².

9-6 Friis Transmission Formula

The two antennas shown in Fig. 9-19 are part of a free-space communication link, with the separation between the antennas, R, being large enough for each antenna to be in the far-field region of the other. The transmitting and receiving antennas have effective areas A_t and A_r and radiation efficiencies ξ_t and ξ_r, respectively. Our objective is to find a relationship between P_t, the transmitter power supplied to the transmitting antenna, and P_{rec}, the power delivered to the receiver by the receiving antenna. As always, we assume that both antennas are impedance matched to their respective transmission lines. Initially, we shall consider the case where the two antennas are oriented such that the peak of the radiation pattern of each antenna points in the direction of the other.

Let us start by treating the transmitting antenna as a lossless isotropic radiator. In this case, the power density incident upon the receiving antenna at a distance R from an isotropic transmitting antenna is simply equal to the transmitter power P_t divided by the surface area of a sphere of radius R:

$$S_{iso} = \frac{P_t}{4\pi R^2}. \quad (9.71)$$

The real transmitting antenna is neither lossless nor isotropic. Hence, the power density S_t due to the real

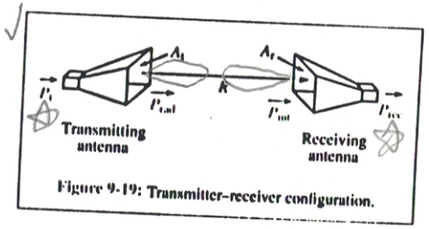

Figure 9-19: Transmitter–receiver configuration.

antenna is given by

$$S_r = G_t S_{iso} = \xi_t D_t S_{iso} = \frac{\xi_t D_t P_t}{4\pi R^2}. \qquad (9.72)$$

where, through the gain $G_t = \xi_t D_t$, ξ_t accounts for the fact that only part of the power P_t supplied to the antenna actually is radiated out into space, and D_t accounts for the directivity of the transmitting antenna (in the direction of the receiving antenna). Using Eq. (9.64), Eq. (9.72) can be expressed in terms of the effective area A_t of the transmitting antenna:

$$S_r = \frac{\xi_t A_t P_t}{\lambda^2 R^2}. \qquad (9.73)$$

On the receiving-antenna side, the power intercepted by the receiving antenna is equal to the product of the incident power density S_r and the effective area A_r:

$$P_{int} = S_r A_r = \frac{\xi_t A_t A_r P_t}{\lambda^2 R^2}. \qquad (9.74)$$

The received power P_{rec} delivered to the receiver is equal to the intercepted power P_{int} multiplied by the radiation efficiency of the receiving antenna, ξ_r. Thus, $P_{rec} = \xi_r P_{int}$, which leads to the result

$$\boxed{\frac{P_{rec}}{P_t} = \frac{\xi_t \xi_r A_t A_r}{\lambda^2 R^2} = G_t G_r \left(\frac{\lambda}{4\pi R}\right)^2}. \qquad (9.75)$$

This relation is known as the *Friis transmission formula*, and P_{rec}/P_t is sometimes called the *power transfer ratio*. In deriving the form of the Friis formula involving the gains G_t and G_r of the transmitting and receiving antennas, we used the fact that $\xi_t A_t = \xi_t D_t \lambda^2/4\pi = G_t \lambda^2/4\pi$, and similar relations apply to the receiving antenna.

If the two antennas are not oriented in the direction of maximum power transfer, Eq. (9.75) can be rewritten in the general form

$$\frac{P_{rec}}{P_t} = G_t G_r \left(\frac{\lambda}{4\pi R}\right)^2 F_t(\theta_t, \phi_t)\, F_r(\theta_r, \phi_r), \qquad (9.76)$$

where $F_t(\theta_t, \phi_t)$ is the normalized radiation intensity of the transmitting antenna, evaluated at the direction (θ_t, ϕ_t) corresponding to the direction of the receiving antenna (as seen by the antenna pattern of the transmitting antenna), and a similar definition applies to $F_r(\theta_r, \phi_r)$ for the receiving antenna.

Example 9-8 Satellite Communication System

A 6-GHz direct-broadcast TV satellite system transmits 100 W through a 2-m-diameter parabolic dish antenna from a distance of approximately 40,000 km above Earth's surface. Each TV channel occupies a bandwidth of 5 MHz. Due to electromagnetic noise picked up by the antenna as well as noise generated by the receiver electronics, a ground home receiving TV station has a noise level given by

$$P_n = K T_{sys} B \quad \text{(W)}, \qquad (9.77)$$

where T_{sys} [measured in kelvins (K)] is a figure of merit, called the *system noise temperature*, that characterizes the noise performance of the receiver–antenna combination, K is Boltzmann's constant [1.38×10^{-23} (J/K)], and B is the receiver bandwidth in Hz.

The *signal-to-noise ratio* S_n (which should not be confused with the power density S) is defined as the ratio of P_{rec}, the signal power received from the transmitter, to P_n:

$$S_n = P_{rec}/P_n \quad \text{(dimensionless)}. \qquad (9.78)$$

For a receiver with $T_{sys} = 580$ K, what minimum diameter of a parabolic dish receiving antenna is required for high-quality TV reception with $S_n = 40$ dB? The satellite and ground receiving antennas may be assumed lossless, and their effective areas may be assumed equal to their physical apertures.

Solution: The following quantities are given:

$$P_t = 100 \text{ W}, \quad f = 6 \text{ GHz} = 6 \times 10^9 \text{ Hz}, \quad S_n = 10^4.$$

Transmit antenna diameter $d_t = 2$ m,

$$T_{sys} = 580 \text{ K},$$
$$R = 40{,}000 \text{ km} = 4 \times 10^7 \text{ m},$$
$$B = 5 \text{ MHz} = 5 \times 10^6 \text{ Hz}.$$

The wavelength $\lambda = c/f = 5 \times 10^{-2}$ m, and the area of the transmitting satellite antenna is $A_t = (\pi d_t^2/4) = \pi$ (m^2). From Eq. (9.77), the receiver noise power is

$$P_n = K T_{sys} B = 1.38 \times 10^{-23} \times 580 \times 5 \times 10^6 = 4 \times 10^{-14} \text{ W}.$$

Using Eq. (9.75) for lossless antennas ($\xi_t = \xi_r = 1$), the received signal power is

$$P_{rec} = \frac{P_t A_t A_r}{\lambda^2 R^2} = \frac{100\pi A_r}{(5 \times 10^{-2})^2 (4 \times 10^7)^2} = 7.85 \times 10^{-11} A_r.$$

The area of the receiving antenna, A_r, can now be determined by equating the ratio P_{rec}/P_n to $S_n = 10^4$:

$$10^4 = \frac{7.85 \times 10^{-11} A_r}{4 \times 10^{-14}},$$

which yields the value $A_r = 5.1$ m^2. The required minimum diameter is $d_r = \sqrt{4A_r/\pi} = 2.55$ m. ■

EXERCISE 9.8 Suppose that the operating frequency of the communication system described in Example 9-5 were to be doubled to 12 GHz. What would then be the minimum required diameter of a home receiving TV antenna?

Ans. $d_r = 1.27$ m.

EXERCISE 9.9 A 3-GHz microwave link consists of two identical antennas each with a gain of 30 dB. If the transmitter output power is 1 kW and the two antennas are 10 km apart, find the received power.

Ans. $P_{rec} = 6.33 \times 10^{-4}$ W.

EXERCISE 9.10 The effective area of a parabolic dish antenna is approximately equal to its physical aperture. If the directivity of a dish antenna is 30 dB at 10 GHz, what is its effective area? If the frequency is increased to 30 GHz, what will be its new directivity?

Ans. $A_e = 0.07$ m^2, $D = 39.54$ dB.

9-7 Radiation by Large-Aperture Antennas

For wire antennas, the sources of radiation are the infinitesimal current elements comprising the current distribution along the wire, and the total radiated field at a given point in space is equal to the sum, or integral, of the fields radiated by all the elements. A parallel arrangement applies to aperture antennas, except that now the source of radiation is the electric-field distribution across the aperture. Consider the horn antenna shown in Fig. 9-20, which is connected to a source through a coaxial transmission line, with the outer conductor of the coaxial line being connected to the metal body of the horn and the inside conductor made to protrude, through a small hole, partially into the throat end of the horn. The protruding conductor acts as a monopole antenna, generating waves that radiate outwardly toward

REVIEW QUESTIONS

Q9.11 For an a-c generator connected to a load, what is the condition for maximum transfer of power from the generator to the load?

Q9.12 If the two antennas of a communication system have constant radiation efficiencies and effective areas, how does the power transfer ratio vary with λ? Explain in terms of how the antenna beams vary with λ.

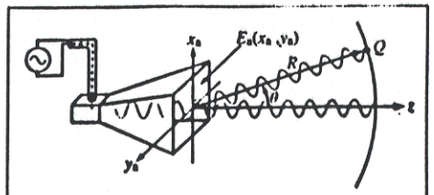

Figure 9-20: A horn antenna with aperture field distribution $E_a(x_a, y_a)$.

the horn's aperture. The electric field of the energy arriving at the aperture, which may vary as a function of x_a and y_a over the horn's aperture, is called the electric-field aperture distribution, $E_a(x_a, y_a)$. Inside the horn, wave propagation is guided by the horn's geometry; but as the wave transitions from a guided wave into an unbounded wave, every point of its wavefront serves as a source of spherical secondary wavelets. The aperture may then be represented as a distribution of isotropic radiators, each with an intensity proportional to the electric field $E_a(x_a, y_a)$ at its location (x_a, y_a). At a distant point Q, the combination of all the waves arriving from all of these radiators constitutes the total wave that would be observed by a receiver placed at that point.

The radiation process described for the horn antenna is equally applicable to any aperture upon which an electromagnetic wave is incident. For example, if a light source is used to illuminate an opening in an opaque screen through a collimating lens, as shown in Fig. 9-21(a), the opening becomes a source of secondary spherical wavelets, much like the aperture of the horn antenna. In the case of the parabolic reflector shown in Fig. 9-21(b), it can be described in terms of an imaginary aperture representing the electric-field distribution across a plane in front of the reflector.

Two types of mathematical formulations are available for computing the electromagnetic fields of waves radiated by apertures. The first type is a *scalar formulation* based on Kirchhoff's work and is used commonly in optical diffraction problems and for large-aperture

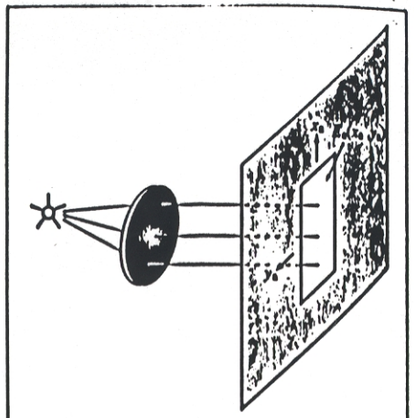

(a) Opening in an opaque screen

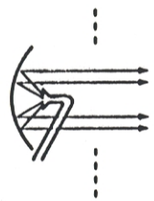

(b) Parabolic reflector antenna

Figure 9-21: Radiation by apertures: (a) an opening in an opaque screen illuminated by a light source through a collimating lens and (b) a parabolic dish reflector illuminated by a small horn antenna.

antennas. The second type is a *vector formulation* based on Maxwell's equations. Although theoretically superior, the vector approach generally is more difficult to apply. Hence, it is used mostly in connection with antenna apertures whose dimensions are comparable to or smaller than a wavelength, because in this case the scalar approach is inapplicable.

In this section, we shall limit our presentation to the scalar diffraction approach, in part because of its inherent simplicity and also because it is applicable to a wide range of practical applications. *The key requirement for the validity of the scalar formulation is that the antenna aperture be at least several wavelengths long along each of its principal dimensions.* A distinctive feature of such an antenna is its high directivity and correspondingly narrow beam, which makes it attractive for radar and free-space microwave communication systems. The frequency range commonly used for these applications is the 1- to 30-GHz microwave band. Because the corresponding wavelength range is 30 to 1 cm, respectively, it is quite practical to construct and use antennas (in this frequency range) with aperture dimensions that are many wavelengths in size.

The x_a–y_a plane in Fig. 9-22, denoted plane A, contains an aperture with an electric field distribution $E_a(x_a, y_a)$, usually called the *aperture illumination*. For the sake of convenience, the opening has been chosen to be rectangular in shape, with dimensions l_x along x_a and l_y along y_a, even though the formulation we are about to discuss is general enough to accommodate any two-dimensional aperture distribution, including those associated with circular and elliptical apertures. At a distance z from the aperture plane A in Fig. 9-22, we have an observation plane O with axes (x, y). The two planes have parallel axes and are separated by a distance z that is sufficiently large so that any point Q in the observation plane is in the far-field region of the aperture. To satisfy the far-field condition, it is necessary that

$$R \geq 2d^2/\lambda, \quad (9.79)$$

where d is the longest linear dimension of the radiating aperture.

The position of observation point Q is specified by the range R between the center of the aperture and point Q and by the angles θ and ϕ shown in Fig. 9-22, which together define the direction of the observation point relative to the coordinate system of the aperture. The electric field phasor of the wave incident upon point Q is denoted $\tilde{E}(R, \theta, \phi)$. Kirchhoff's scalar diffraction theory provides the following relationship between the radiated field $\tilde{E}(R, \theta, \phi)$ and the aperture illumination $\tilde{E}_a(x_a, y_a)$:

$$\tilde{E}(R, \theta, \phi) = \frac{j}{\lambda}\left(\frac{e^{-jkR}}{R}\right)\tilde{h}(\theta, \phi), \quad (9.80)$$

where

$$\tilde{h}(\theta, \phi) = \iint_{-\infty}^{\infty} \tilde{E}_a(x_a, y_a) \cdot \exp[jk \sin\theta(x_a \cos\phi + y_a \sin\phi)]\, dx_a\, dy_a. \quad (9.81)$$

We shall refer to $\tilde{h}(\theta, \phi)$ as the *form factor* of $\tilde{E}(R, \theta, \phi)$. Its integral is written with infinite limits, with the understanding that $\tilde{E}_a(x_a, y_a)$ is identically zero outside the aperture. The spherical propagation factor (e^{-jkR}/R) accounts for wave propagation between the center of the aperture and the observation point, and $\tilde{h}(\theta, \phi)$ represents an integration of the exciting field $\tilde{E}_a(x_a, y_a)$ over the extent of the aperture, taking into account [through the exponential function in Eq. (9.81)] the approximate deviation in distance between R and s, where s is the distance to any point (x_a, y_a) in the aperture plane [see Fig. 9-22]. *The polarization direction of the radiated field $\tilde{E}(R, \theta, \phi)$ is the same as that of the aperture field*

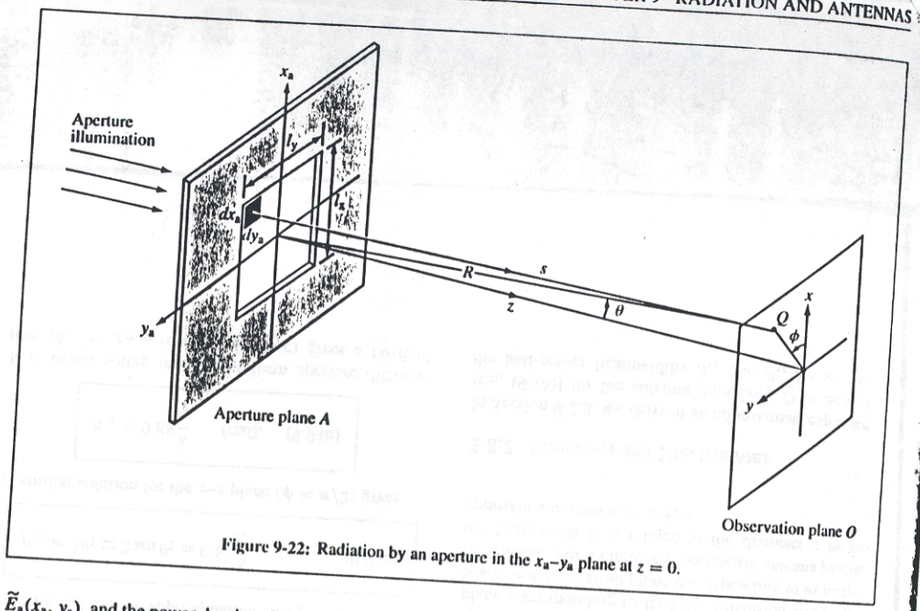

Figure 9-22: Radiation by an aperture in the x_a–y_a plane at $z = 0$.

$\widetilde{E}_a(x_a, y_a)$, and the power density of the radiated wave is given by

$$S(R, \theta, \phi) = \frac{|\widetilde{E}(R, \theta, \phi)|^2}{2\eta_0} = \frac{|\widetilde{h}(\theta, \phi)|^2}{2\eta_0 \lambda^2 R^2}. \quad (9.82)$$

$= S_0 \operatorname{sinc}^2(\pi l_x \sin\theta/\lambda)$

9-8 Rectangular Aperture with Uniform Aperture Distribution

By way of illustrating the scalar diffraction technique, let us consider a rectangular aperture of height l_x and width l_y, both at least a few wavelengths long. The aperture is excited by a uniform field distribution given by

$$\widetilde{E}_a(x_a, y_a) = \begin{cases} E_0, & \text{for } -l_x/2 \le x_a \le l_x/2 \\ & \text{and } -l_y/2 \le y_a \le l_y/2, \\ 0, & \text{otherwise.} \end{cases} \quad (9.83)$$

To keep the mathematics simple, let us confine our examination to the radiation pattern at a fixed range R in the x–z plane, corresponding to $\phi = 0$. In this case, Eq. (9.81) simplifies to

$$\widetilde{h}(\theta) = \int_{y_a=-l_y/2}^{l_y/2} \int_{x_a=-l_x/2}^{l_x/2} E_0 \exp[jkx_a \sin\theta]\, dx_a\, dy_a. \quad (9.84)$$

In preparation for performing the integration in Eq. (9.84), we introduce the intermediate variable u defined as

$$u = k \sin\theta = \frac{2\pi \sin\theta}{\lambda}, \quad (9.85)$$

in which case Eq. (9.84) becomes

$$\begin{aligned} \widetilde{h}(\theta) &= E_0 \int_{-l_x/2}^{l_x/2} e^{jux_a}\, dx_a \cdot \int_{-l_y/2}^{l_y/2} dy_a \\ &= E_0 \left[\frac{e^{jul_x/2} - e^{-jul_x/2}}{ju}\right] \cdot l_y \\ &= \frac{2E_0 l_y}{u} \left[\frac{e^{jul_x/2} - e^{-jul_x/2}}{2j}\right] \\ &= \frac{2E_0 l_y}{u} \sin(ul_x/2). \end{aligned} \quad (9.86)$$

Upon replacing u with its defining expression, we have

$$\begin{aligned} \widetilde{h}(\theta) &= \frac{2E_0 l_y}{\left(\frac{2\pi}{\lambda} \sin\theta\right)} \sin(\pi l_x \sin\theta/\lambda) \\ &= E_0 l_x l_y \frac{\sin(\pi l_x \sin\theta/\lambda)}{\pi l_x \sin\theta/\lambda} \\ &= E_0 A_p \operatorname{sinc}(\pi l_x \sin\theta/\lambda), \end{aligned} \quad (9.87)$$

where $A_p = l_x l_y$ is the physical area of the aperture and where we have used the standard definition of the sinc function, which, for any argument t, is defined as

$$\operatorname{sinc} t = \frac{\sin t}{t}. \quad (9.88)$$

Using Eq. (9.82), we obtain the following expression for the power density of the radiated wave at the observation point:

$$S(R, \theta) = S_0 \operatorname{sinc}^2(\pi l_x \sin\theta/\lambda) \quad (x\text{–}z \text{ plane}), \quad (9.89)$$

where $S_0 = E_0^2 A_p^2/(2\eta_0 \lambda^2 R^2)$. The sinc function is at a maximum when its argument is equal to zero and its value is equal to unity. This occurs when $\theta = 0$. Thus, at a fixed range R, $S_{max} = S(\theta = 0) = S_0$. The normalized radiation intensity is then given by

$$\begin{aligned} F(\theta) &= \frac{S(R, \theta)}{S_{max}} \\ &= \operatorname{sinc}^2(\pi l_x \sin\theta/\lambda) \\ &= \operatorname{sinc}^2(\pi\gamma) \quad (x\text{–}z \text{ plane}), \end{aligned} \quad (9.90)$$

and it is plotted (on a decibel scale) in Fig. 9-23 as a function of the intermediate variable $\gamma = (l_x/\lambda) \sin\theta$. The pattern exhibits nulls at nonzero integer values of γ.

9-8.1 Beamwidth

The normalized radiation intensity $F(\theta)$ is symmetrical in the x–z plane, and its maximum is along the boresight direction ($\theta = 0$, in this case). Its half-power beamwidth $\beta_{xz} = \theta_2 - \theta_1$, where θ_1 and θ_2 are the values of θ at which $F(\theta, 0) = 0.5$ (or -3 dB on a decibel scale), as shown in Fig. 9-23. Since the pattern is symmetrical with respect to $\theta = 0$, $\theta_1 = -\theta_2$ and $\beta_{xz} = 2\theta_2$. The angle θ_2 can be obtained from a solution of

$$F(\theta_2) = \operatorname{sinc}^2(\pi l_x \sin\theta/\lambda) = 0.5. \quad (9.91)$$

From tabulated values of the sinc function, it is found that Eq. (9.91) yields the result

$$\frac{\pi l_x}{\lambda} \sin\theta_2 = 1.39, \quad (9.92)$$

or

$$\sin\theta_2 = 0.44 \frac{\lambda}{l_x}. \quad (9.93)$$

Because $\lambda/l_x \ll 1$ (a fundamental condition of scalar diffraction theory is that the aperture dimensions be much

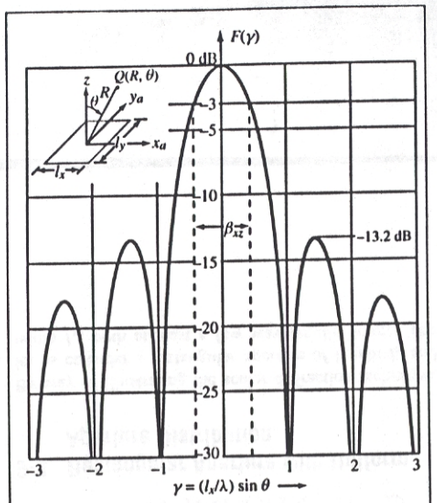

Figure 9-23: Normalized radiation pattern of a uniformly illuminated rectangular aperture in the x–z plane ($\phi = 0$).

larger than the wavelength λ), θ_2 is a small angle, in which case we can use the approximation $\sin\theta_2 \simeq \theta_2$. Hence,

$$\beta_{xz} = 2\theta_2 \simeq 2\sin\theta_2 = 0.88\frac{\lambda}{l_x} \quad \text{(rad)}. \qquad (9.94a)$$

A similar solution for the y–z plane ($\phi = \pi/2$) gives

$$\beta_{yz} = 0.88\frac{\lambda}{l_y} \quad \text{(rad)}. \qquad (9.94b)$$

It is worth noting that the uniform aperture distribution ($\widetilde{E}_a = E_0$ across the aperture) gives a far-field pattern with the narrowest possible beamwidth. The first sidelobe level is 13.2 dB below the peak value [see Fig. 9-23], which is equivalent to 4.8% of the peak value. If the intended application calls for a pattern with a lower sidelobe level (to avoid interference with signals from sources along directions outside the main beam of the antenna pattern), this can be accomplished by using a *tapered aperture distribution*, one that is a maximum at the center of the aperture and decreases toward the edges. A tapered distribution provides a pattern with lower side lobes, but the main lobe becomes wider. The steeper the taper, the lower are the side lobes and the wider is the main lobe. In general, the beamwidth in a given plane, say the x–z plane, is given by

$$\beta_{xz} = k_x\frac{\lambda}{l_x}, \qquad (9.95)$$

where k_x is a constant related to the steepness of the taper. For a uniform distribution with no taper, $k_x = 0.88$, and for a highly tapered distribution, $k_x \simeq 2$. In the typical case, $k_x \simeq 1$.

To illustrate the relationship between the antenna dimensions and the corresponding beam shape, we show in Fig. 9-24 the radiation patterns of a circular reflector and a cylindrical reflector. The circular reflector has a circularly symmetric pattern, whereas the pattern of the cylindrical reflector has a narrow beam in the azimuth plane corresponding to its long dimension and a wide beam in the elevation plane corresponding to its narrow dimension. For a circularly symmetric antenna pattern, the beamwidth β is related to the diameter d by the approximate relation $\beta \simeq \lambda/d$.

9-8.2 Directivity and Effective Area

In Section 9-2.3, we derived an approximate expression [Eq. (9.26)] for the antenna directivity D in terms of the half-power beamwidths β_{xz} and β_{yz} for antennas

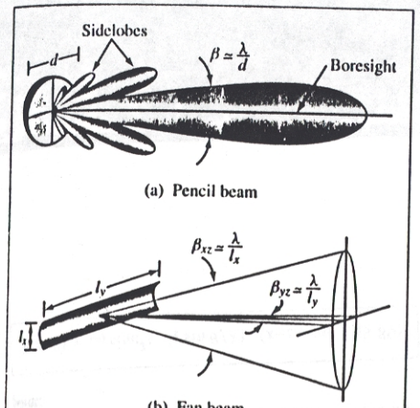

Figure 9-24: Radiation patterns of (a) a circular reflector and (b) a cylindrical reflector (side lobes not shown).

characterized by a single major lobe whose boresight is along the z-direction:

$$D \simeq \frac{4\pi}{\beta_{xz}\beta_{yz}}. \qquad (9.96)$$

If we use the approximate relations $\beta_{xz} \simeq \lambda/l_x$ and $\beta_{yz} \simeq \lambda/l_y$, we have

$$D \simeq \frac{4\pi l_x l_y}{\lambda^2} = \frac{4\pi A_p}{\lambda^2}. \qquad (9.97)$$

For any antenna, its directivity is related to its effective area A_e by Eq. (9.64):

$$D = \frac{4\pi A_e}{\lambda^2}. \qquad (9.98)$$

Hence, *for aperture antennas, their effective apertures are approximately equal to their physical apertures;* that is, $A_e \simeq A_p$.

EXERCISE 9.11 Verify that Eq. (9.92) is a solution of Eq. (9.91) by calculating $\text{sinc}^2 t$ for $t = 1.39$.

EXERCISE 9.12 With its boresight direction along z, a square aperture was observed to have half-power beamwidths of 3° in both the x–z and y–z planes. Determine its directivity in decibels.

Ans. $D = 4{,}583.66 = 36.61$ dB.

EXERCISE 9.13 What condition must be satisfied in order to use scalar diffraction to compute the field radiated by an aperture antenna? Can we use it to compute the directional pattern of the eye's pupil ($d \cong 0.2$ cm) in the visible part of the spectrum ($\lambda = 0.35$ to $0.7\ \mu$m)? What would the beamwidth of the eye's directional pattern be at $\lambda = 0.5\ \mu$m if we assume that the pupil is uniformly illuminated?

Ans. $\beta = 0.88\ \lambda/d = 2.2 \times 10^{-4}$ rad $= 0.76'$ (arc minute, with $60' = 1°$).

9-9 Antenna Arrays

AM broadcast services operate in the 535- to 1605-kHz band. The antennas they use are basically vertical dipoles mounted along tall towers. The antennas range in height from $\lambda/6$ to $5\lambda/8$, depending on the operating characteristics desired and other considerations. Their physical heights vary from 46 m (150 ft) to 274 m (900 ft); the wavelength at 1 MHz, approximately in the middle of the AM band, is 300 m. Because the field radiated by a single dipole is uniform in the horizontal plane (as discussed in Sections 9-1 and 9-3), it is necessary to use more than one antenna tower to direct the horizontal antenna pattern along directions of interest (such as a city)

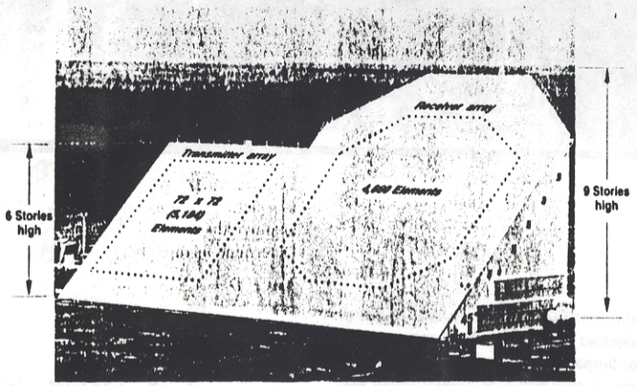

Figure 9-25: The AN/FPS-85 Phased Array Radar Facility in the Florida panhandle, near the city of Freeport. A several-mile no-fly zone surrounds the radar installation as a safety concern for electroexplosive devices, such as ejection seats and munitions, carried on military aircraft.

and to minimize it along directions of low population density or a direction corresponding to an area serviced by another station operating at the same frequency (to avoid undesirable interference effects). When two or more antennas are used together, the combination is called an *antenna array*.

The AM broadcast antenna array is only one application example of antenna arrays; they are used extensively in numerous communication systems and radar applications as well. Antenna arrays provide the antenna designer the flexibility to obtain high directivity, narrow beams, low side lobes, steerable beams, and shaped antenna patterns. Figure 9-25 shows a photograph of a very large radar system consisting of a transmitter array composed of 5,184 individual dipole antenna elements and a receiver array composed of 4,660 elements. The radar system, part of the Space Surveillance Network operated by the U.S. Air Force, operates at 442 MHz and transmits a combined peak power of 30 MW!

Although an array need not consist of similar radiating elements, most arrays usually use identical elements, such as dipoles, slots, horn antennas, or parabolic dishes, excited by the same type of current or field distribution. The antenna elements comprising an array may be arranged in various configurations, but the most common are the linear one-dimensional configuration, wherein the elements are arranged along a straight line, and the two-dimensional lattice configuration, wherein the elements

form a rectangular grid. The desired shape of the far-field radiation pattern of the array can be synthesized by controlling the relative amplitudes of the array elements. Also, through the use of electronically controlled solid-state phase shifters, the beam direction of the antenna array can be steered electronically by controlling the relative phases of the array elements. This flexibility of the array antenna has led to numerous applications, including *electronic steering* and *multiple-beam generation*.

The purpose of this and the next two sections is to introduce the reader to the basic principles of array theory and to the design techniques used in shaping the antenna pattern and steering the main lobe. The presentation will be confined to the one-dimensional linear array with equal spacing between adjacent elements.

A linear array of N identical radiators is arranged along the z-axis as shown in Fig. 9-26. The radiators are fed by a common oscillator through a branching network. In each branch, an attenuator (or amplifier) and phase shifter are inserted in series to control the amplitude and phase of the signal feeding the antenna element in that branch.

In the far-field region of any radiating element, the phasor electric-field intensity $\widetilde{E}_e(R, \theta, \phi)$ may be expressed as a product of two functions, the spherical propagation factor e^{-jkR}/R, which accounts for the dependence on the range R, and $\widetilde{f}_e(\theta, \phi)$, which accounts for the directional dependence of the element's electric field. Thus, for an isolated element, the radiated field is

$$\widetilde{E}_e(R, \theta, \phi) = \frac{e^{-jkR}}{R} \widetilde{f}_e(\theta, \phi), \qquad (9.99)$$

and the corresponding power density S_e is

$$S_e(R, \theta, \phi) = \frac{1}{2\eta_0} |\widetilde{E}_e(R, \theta, \phi)|^2 = \frac{1}{2\eta_0 R^2} |\widetilde{f}_e(\theta, \phi)|^2. \qquad (9.100)$$

With regard to the elements in the array shown in Fig. 9-26(b), the far-zone field due to element i at range R_i

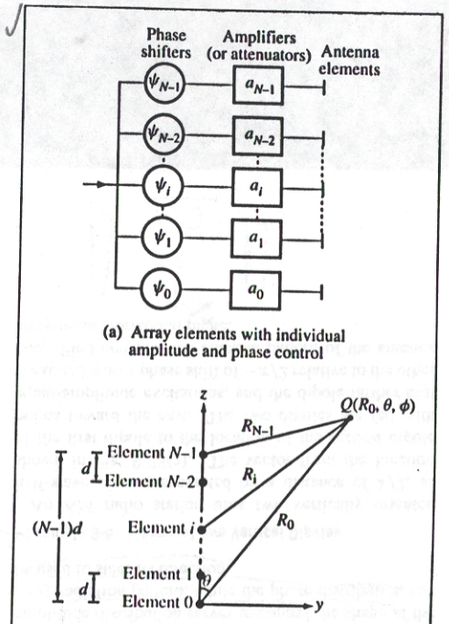

Figure 9-26: Linear-array configuration and geometry.

from the observation point Q may then be written in the form

$$\widetilde{E}_i(R_i, \theta, \phi) = A_i \frac{e^{-jkR_i}}{R_i} \widetilde{f}_e(\theta, \phi), \qquad (9.101)$$

where $A_i = a_i e^{j\psi_i}$ is a *complex feeding coefficient* representing the amplitude a_i and phase ψ_i of the excitation

giving rise to $\widetilde{E}_i$, relative to a reference excitation. In practice, the excitation of one of the elements is used as reference. Note that R_i and A_i may be different for the different elements in the array, but $\widetilde{f}_e(\theta, \phi)$ is the same for all the elements since they are assumed to be identical and hence exhibit identical directional patterns.

The total field at the observation point $Q(R_0, \theta, \phi)$ is the sum of the fields due to the N elements:

$$\widetilde{E}(R_0, \theta, \phi) = \sum_{i=0}^{N-1} \widetilde{E}_i(R_i, \theta, \phi) = \left[\sum_{i=0}^{N-1} A_i \frac{e^{-jkR_i}}{R_i}\right] \widetilde{f}_e(\theta, \phi), \quad (9.102)$$

where R_0 denotes the range of Q from the center of the coordinate system, chosen to be at the location of the zeroth element. To satisfy the far-field condition given by Eq. (9.79) for an array of length $l = (N-1)d$, where d is the interelement spacing, the range R_0 should be sufficiently large that

$$R_0 \geq \frac{2l^2}{\lambda} = \frac{2(N-1)^2 d^2}{\lambda}. \quad (9.103)$$

This condition allows us to ignore differences in the distances from Q to the individual elements as far as the magnitude of the radiated field is concerned. Thus, we can set $R_i = R_0$ in the denominator in Eq. (9.102) for all i. With regard to the phase part of the propagation factor, we can use the parallel-ray approximation given by

$$R_i \simeq R_0 - z_i \cos\theta = R_0 - id\cos\theta, \quad (9.104)$$

where $z_i = id$ is the distance between the ith element and the zeroth element [Fig. 9-27]. Employing these two approximations in Eq. (9.102) leads to

$$\widetilde{E}(R_0, \theta, \phi) = \widetilde{f}_e(\theta, \phi)\left(\frac{e^{-jkR_0}}{R_0}\right) \times \left[\sum_{i=0}^{N-1} A_i e^{jikd\cos\theta}\right], \quad (9.105)$$

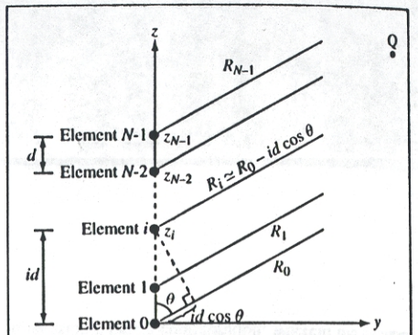

Figure 9-27: The rays between the elements and a faraway observation point are approximately parallel lines. Hence, the distance $R_i \simeq R_0 - id\cos\theta$.

and the corresponding array-antenna power density is given by

$$S(R_0, \theta, \phi) = \frac{1}{2\eta_0}|\widetilde{E}(R_0, \theta, \phi)|^2 = \frac{1}{2\eta_0 R_0^2}|\widetilde{f}_e(\theta, \phi)|^2 \left|\sum_{i=0}^{N-1} A_i e^{jikd\cos\theta}\right|^2 = S_e(R_0, \theta, \phi)\left|\sum_{i=0}^{N-1} A_i e^{jikd\cos\theta}\right|^2, \quad (9.106)$$

where use has been made of Eq. (9.100). This expression is a product of two factors. The first factor, $S_e(R_0, \theta, \phi)$, is the power density of the energy radiated by an individual element, and the second, usually called the *array factor*, is a function of the positions of the individual elements and their feeding coefficients, but not a function of the specific type of radiators used. *The array factor represents the far-field radiation intensity of the N elements, had the elements been isotropic radiators.* Denoting the array factor by

$$F_a(\theta) = \left|\sum_{i=0}^{N-1} A_i e^{jikd\cos\theta}\right|^2, \quad (9.107)$$

the power density of the antenna array is then written as

$$S(R_0, \theta, \phi) = S_e(R_0, \theta, \phi)\, F_a(\theta). \quad (9.108)$$

This equation is called the *pattern multiplication principle*. It allows us to find the far-field power density of the antenna array by first computing the far-field power pattern with the array elements replaced with isotropic radiators, which yields the array factor $F_a(\theta)$, and then multiplying the result by $S_e(R_0, \theta, \phi)$, the power density for a single element (which should be the same for all the elements).

The feeding coefficient A_i is, in general, a complex amplitude consisting of an amplitude factor a_i and a phase factor ψ_i:

$$A_i = a_i e^{j\psi_i}. \quad (9.109)$$

Insertion of Eq. (9.109) into Eq. (9.107) leads to

$$F_a(\theta) = \left|\sum_{i=0}^{N-1} a_i e^{j\psi_i} e^{jikd\cos\theta}\right|^2. \quad (9.110)$$

The array factor is governed by two input functions: the *array amplitude distribution* given by the a_i's and the *array phase distribution* given by the ψ_i's. The amplitude distribution serves to control the shape of the array radiation pattern, while the phase distribution can be used to steer its direction.

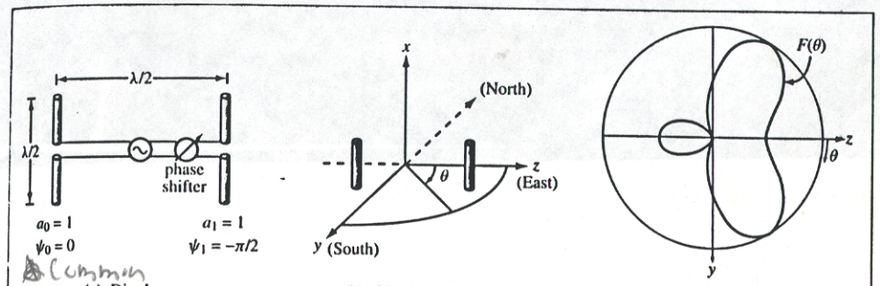

Figure 9-28: Two half-wave dipole array of Example 9-6.

Example 9-6 Array of Two Vertical Dipoles

An AM radio station uses two vertically oriented half-wave dipoles separated by a distance of $\lambda/2$, as shown in Fig. 9-28(a). The vector from the location of the first dipole to the location of the second dipole points toward the east. The two dipoles are fed with equal-amplitude excitations, and the dipole farther east is excited with a phase shift of $-\pi/2$ relative to the other one. Find and plot the antenna pattern of the antenna array in the horizontal plane.

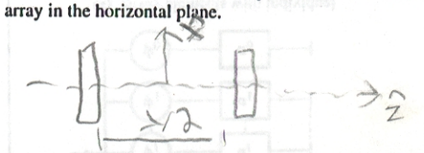

Solution: The array factor given by Eq. (9.110) was derived for radiators arranged along the z-axis. To keep the coordinate system the same, we choose the easterly direction to be the z-axis as shown in Fig. 9-28(b), and we place the first dipole at $z = -\lambda/4$ and the second at $z = \lambda/4$. A half-wave dipole radiates uniformly in the plane perpendicular to its axis, which in this case is the horizontal plane. Hence, $S_e = S_0$ for all angles θ in Fig. 9-28(b), where S_0 is the maximum value of the power density radiated by each dipole individually. Consequently, the power density radiated by the two-dipole array is

$$S(R, \theta) = S_0 F_a(\theta).$$

For two elements separated by $d = \lambda/2$ and excited with equal amplitudes ($a_0 = a_1 = 1$) and with phase angles $\psi_0 = 0$ and $\psi_1 = -\pi/2$, Eq. (9.110) gives

$$\begin{aligned} F_a(\theta) &= \left| \sum_{i=0}^{1} a_i e^{j\psi_i} e^{jikd\cos\theta} \right|^2 \\ &= |1 + e^{-j\pi/2} e^{j(2\pi/\lambda)(\lambda/2)\cos\theta}|^2 \\ &= |1 + e^{j(\pi\cos\theta - \pi/2)}|^2. \end{aligned}$$

A function of the form $|1 + e^{jx}|^2$ can be evaluated by factoring out $e^{jx/2}$ from both terms:

$$\begin{aligned} |1 + e^{jx}|^2 &= |e^{jx/2}(e^{-jx/2} + e^{jx/2})|^2 \\ &= |e^{jx/2}|^2 \, |e^{-jx/2} + e^{jx/2}|^2 \\ &= |e^{jx/2}|^2 \left| 2\frac{[e^{-jx/2} + e^{jx/2}]}{2} \right|^2. \end{aligned}$$

The absolute value of $e^{jx/2}$ is equal to 1, and we recognize the function inside the square bracket as $\cos(x/2)$. Hence,

$$|1 + e^{jx}|^2 = 4\cos^2\left(\frac{x}{2}\right).$$

Applying this result to the expression for $F_a(\theta)$, we have

$$F_a(\theta) = 4\cos^2\left(\frac{\pi}{2}\cos\theta - \frac{\pi}{4}\right).$$

The power density radiated by the array is then

$$S(R, \theta) = S_0 F_a(\theta) = 4S_0 \cos^2\left(\frac{\pi}{2}\cos\theta - \frac{\pi}{4}\right).$$

This function has a maximum value $S_{max} = 4S_0$, and it occurs when the argument of the cosine function is equal to zero. Thus,

$$\frac{\pi}{2}\cos\theta - \frac{\pi}{4} = 0,$$

which leads to the solution: $\theta = 60°$. Upon normalizing $S(R, \theta)$ by its maximum value, we obtain the normalized radiation intensity given by

$$F(\theta) = \frac{S(R, \theta)}{S_{max}} = \cos^2\left(\frac{\pi}{2}\cos\theta - \frac{\pi}{4}\right).$$

The pattern of $F(\theta)$ is shown in Fig. 9-28(c). ■

Example 9-7 Pattern Synthesis

In Example 9-6, we were given the array parameters a_0, a_1, ψ_0, ψ_1, and d, and we were then asked to determine the pattern of the two-element dipole array. We will now consider the reverse process; we will be given specifications on the desired pattern, and we are then asked to specify the array parameters to meet those specifications.

Given two vertical dipoles, as depicted in Fig. 9-28(b), specify the array parameters such that the array exhibits maximum radiation toward the east and no radiation toward the north or south.

Solution: From Example 9-6, we established that because each dipole radiates equally along all directions in the y–z plane, the radiation pattern of the two-dipole array in that plane is governed solely by the array factor $F_a(\theta)$. The shape of the pattern of the array factor depends on three parameters: the amplitude ratio a_1/a_0, the phase difference $\psi_1 - \psi_0$, and the spacing d

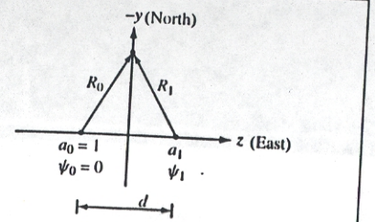

(a) Array arrangement

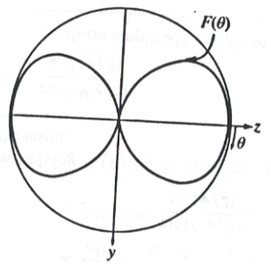

(b) Array pattern

Figure 9-29: (a) Two vertical dipoles separated by a distance d along the z-axis; (b) normalized array pattern in the y–z plane for $a_0 = a_1 = 1$, $\psi_1 = \psi_0 = -\pi$, and $d = \lambda/2$.

[Fig. 9-29(a)]. For convenience, we choose $a_0 = 1$ and $\psi_0 = 0$. Accordingly, Eq. (9.107) gives

$$\begin{aligned} F_a(\theta) &= \left| \sum_{i=0}^{1} a_i e^{j\psi_i} e^{jikd\cos\theta} \right|^2 \\ &= |1 + a_1 e^{j\psi_1} e^{j(2\pi d/\lambda)\cos\theta}|^2. \end{aligned}$$

Let us now consider the given specification requiring that F_a be equal to zero when $\theta = 90°$ (north and south directions in Fig. 9-29(a)). For any observation point on the y-axis, the ranges R_0 and R_1 shown in Fig. 9-29(a) are equal, which means that the propagation phases associated with the time travel of the waves radiated by the two dipoles to that point are identical. Hence, to satisfy the stated condition, we need to choose $a_1 = a_0$ and $\psi_1 = \pm\pi$. With these choices, the signals radiated by the two dipoles will have equal amplitudes and opposite phases, thereby interfering destructively. This conclusion can be ascertained by evaluating the array factor at $\theta = 90°$, with $a_0 = a_1 = 1$ and $\psi_1 = \pm\pi$:

$$F_a(\theta = 90°) = |1 + 1e^{\pm j\pi}|^2 = |1 - 1| = 0.$$

The two values of ψ_1, π and $-\pi$, lead to the same solution for the spacing d when we consider the specification that the array radiation pattern should have a maximum toward the east, corresponding to $\theta = 0°$. Let us choose $\psi_1 = -\pi$ and examine the array factor at $\theta = 0°$:

$$\begin{aligned} F_a(\theta = 0) &= |1 + e^{-j\pi} e^{j2\pi d/\lambda}|^2 \\ &= |1 + e^{j(-\pi + 2\pi d/\lambda)}|^2. \end{aligned}$$

For $F_a(\theta = 0)$ to be a maximum, we require the phase angle of the second term to be zero or a multiple of 2π:

$$-\pi + \frac{2\pi d}{\lambda} = 2n\pi,$$

or

$$d = (2n + 1)\frac{\lambda}{2}, \qquad n = 0, 1, 2, \ldots$$

In summary, the two-dipole array will meet the given specifications if $a_0 = a_1$, $\psi_1 - \psi_0 = -\pi$, and $d = (2n + 1)\lambda/2$.

For $d = \lambda/2$, the array factor at any angle θ is given by

$$\begin{aligned} F_a(\theta) &= |1 + e^{-j\pi} e^{j\pi\cos\theta}|^2 \\ &= |1 - e^{j\pi\cos\theta}|^2 \\ &= \left|2je^{-j(\pi/2)\cos\theta}\left[\frac{e^{j(\pi/2)\cos\theta} - e^{-j(\pi/2)\cos\theta}}{2j}\right]\right|^2 \\ &= 4\sin^2\left(\frac{\pi}{2}\cos\theta\right). \end{aligned}$$

The array factor has a maximum value of 4, which is the maximum level attainable from a two-element array with unit amplitudes. The directions along which $F_a(\theta)$ is a maximum are those corresponding to $\theta = 0$ (east) and $\theta = 180°$ (west), as shown in Fig. 9-29(b). ■

EXERCISE 9.14 Derive an expression for the array factor of a two-element array excited in phase with $a_0 = 1$ and $a_1 = 3$. The elements are positioned along the z-axis and are separated by $\lambda/2$.

Ans. $F_a(\theta) = [10 + 6\cos(\pi\cos\theta)]$.

EXERCISE 9.15 An equally spaced N-element array arranged along the z-axis is fed with equal amplitudes and phases; that is, $A_i = 1$ for $i = 0, 1, \ldots, N-1$. What is the magnitude of the array factor in the broadside direction?

Ans. $F_a(\theta = 90°) = N^2$.

9-10 N-Element Array with Uniform Phase Distribution

We now consider an array of N elements with equal spacing d and equal-phase excitations; that is, $\psi_i = \psi_0$ for $i = 1, 2, \ldots, N-1$. Such an array of in-phase elements is sometimes referred to as a *broadside array* because the main beam of the radiation pattern of its array factor is always in the direction broadside to the array axis. From Eq. (9.110), its array factor is given by

$$\begin{aligned} F_a(\theta) &= \left|e^{j\psi_0}\sum_{i=0}^{N-1} a_i e^{jikd\cos\theta}\right|^2 \\ &= |e^{j\psi_0}|^2\left|\sum_{i=0}^{N-1} a_i e^{jikd\cos\theta}\right|^2 \\ &= \left|\sum_{i=0}^{N-1} a_i e^{jikd\cos\theta}\right|^2. \end{aligned} \tag{9.111}$$

The phase difference between the fields radiated by adjacent elements is

$$\psi = kd\cos\theta = \frac{2\pi d}{\lambda}\cos\theta. \tag{9.112}$$

In terms of ψ, Eq. (9.111) takes the compact form

$$F_a(\psi) = \left|\sum_{i=0}^{N-1} a_i e^{ji\psi}\right|^2 \quad \text{(uniform phase)}. \tag{9.113}$$

For a uniform amplitude distribution with $a_i = 1$ for $i = 0, 1, \ldots, N-1$, Eq. (9.113) becomes

$$F_a(\psi) = |1 + e^{j\psi} + e^{j2\psi} + \cdots + e^{j(N-1)\psi}|^2. \tag{9.114}$$

This geometric series can be rewritten in a more compact form by applying the following procedure. First, we define

$$F_a(\psi) = |f_a(\psi)|^2, \tag{9.115}$$

with

$$f_a(\psi) = [1 + e^{j\psi} + e^{j2\psi} + \cdots + e^{j(N-1)\psi}]. \tag{9.116}$$

Next, we multiply $f_a(\psi)$ by $e^{j\psi}$ to obtain

$$f_a(\psi)\, e^{j\psi} = (e^{j\psi} + e^{j2\psi} + \cdots + e^{jN\psi}). \tag{9.117}$$

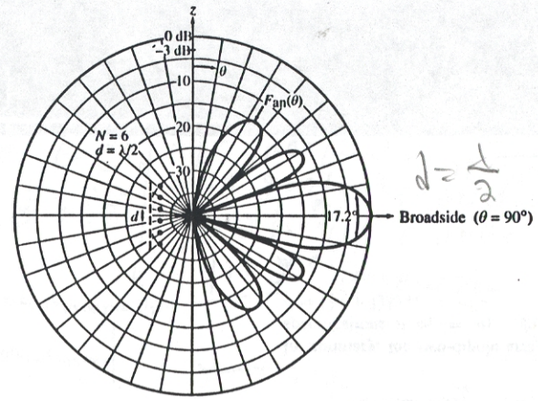

Figure 9-30: Normalized array pattern of a uniformly excited six-element array with interelement spacing $d = \lambda/2$.

Subtracting Eq. (9.117) from Eq. (9.116) gives

$$f_a(\psi)(1 - e^{j\psi}) = 1 - e^{jN\psi}, \tag{9.118}$$

which, in turn, gives

$$\begin{aligned} f_a(\psi) &= \frac{1 - e^{jN\psi}}{1 - e^{j\psi}} \\ &= \frac{e^{jN\psi/2}}{e^{j\psi/2}}\,\frac{(e^{-jN\psi/2} - e^{jN\psi/2})}{(e^{-j\psi/2} - e^{j\psi/2})} \\ &= e^{j(N-1)\psi/2}\,\frac{\sin(N\psi/2)}{\sin(\psi/2)}. \end{aligned} \tag{9.119}$$

After multiplying $f_a(\psi)$ by its complex conjugate, we obtain the result:

$$F_a(\psi) = \frac{\sin^2(N\psi/2)}{\sin^2(\psi/2)} \quad \text{(uniform amplitude and phase)}. \tag{9.120}$$

The maximum value of $F_a(\psi)$ can be shown to occur at $\psi = 0$ (or $\theta = \pi/2$) and is equal to N^2, which is easy to verify by evaluating Eq. (9.114) for $\psi = 0$. Hence, the normalized array factor is given by

$$\begin{aligned} F_{an}(\psi) = \frac{F_a(\psi)}{F_{a,\max}} &= \frac{\sin^2(N\psi/2)}{N^2\sin^2(\psi/2)} \\ &= \frac{\sin^2\left[\frac{N\pi d}{\lambda}\cos\theta\right]}{N^2\sin^2\left[\frac{\pi d}{\lambda}\cos\theta\right]}. \end{aligned} \tag{9.121}$$

A polar plot of $F_{an}(\theta)$ with $N = 6$ is shown in Fig. 9-30 for $d = \lambda/2$. The reader is reminded that this is a plot of the radiation pattern of the array factor alone; the pattern for the antenna array is equal to the product of this pattern and that of a single element, as discussed earlier in connection with the pattern multiplication principle.

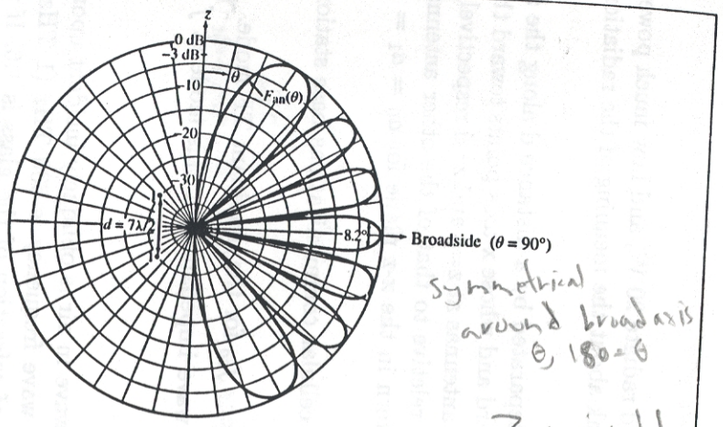

Figure 9-31: Normalized array pattern of a two-element array with spacing $d = 7\lambda/2$.

Example 9-8 Multiple-Beam Array

Obtain an expression for the array factor of a two-element array with equal excitation and a separation $d = 7\lambda/2$, and then plot the array pattern.

Solution: The array factor for a two-element array ($N = 2$) with equal excitation ($a_0 = a_1 = 1$) is given by

$$\begin{aligned} F_a(\gamma) &= \left|\sum_{i=0}^{1} a_i e^{ji\gamma}\right|^2 \\ &= |1 + e^{j\gamma}|^2, \\ &= |e^{j\gamma/2}(e^{-j\gamma/2} + e^{j\gamma/2})|^2 \\ &= |e^{j\gamma/2}|^2\,|e^{-j\gamma/2} + e^{j\gamma/2}|^2 \\ &= 4\cos^2(\gamma/2), \end{aligned}$$

where $\gamma = (2\pi d/\lambda)\cos\theta$. The normalized array pattern, shown in Fig. 9-31, consists of seven beams, all with the same peak value, but not the same angular width. The number of beams in the angular range between $\theta = 0$ and $\theta = \pi$ is equal to the separation between the array elements, d, measured in units of $\lambda/2$. ■

9-11 Electronic Scanning of Arrays

The discussion in the preceding section was concerned with uniform-phase arrays, for which the phases of the feeding coefficients, ψ_0 to ψ_{N-1}, are all equal. In this section, we examine the use of phase delay between adjacent elements as a tool for *electronically steering* the direction of the array-antenna beam from broadside at $\theta = 90°$ to any desired angle θ_0. In addition to eliminating the need to mechanically steer an antenna to change its beam's direction, electronic steering allows beam scanning at very fast rates.

Electronic steering is achieved by applying linearly progressive phase delays from element to element across the array, as shown in Fig. 9-32. Relative to the phase of the zeroth element, the phase of the ith element is

$$\psi_i = -i\delta, \tag{9.122}$$

where δ is the *incremental phase delay* between adjacent elements. Use of Eq. (9.122) in Eq. (9.110) leads to

$$F_a(\theta) = \left|\sum_{i=0}^{N-1} a_i e^{-j i\delta} e^{jikd\cos\theta}\right|^2$$

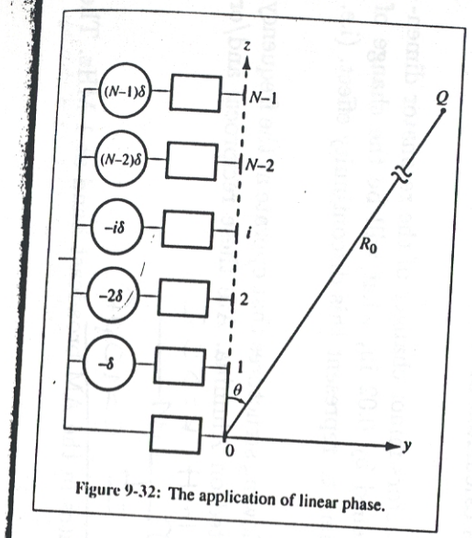

Figure 9-32: The application of linear phase.

$$= \left|\sum_{i=0}^{N-1} a_i e^{ji(kd\cos\theta - \delta)}\right|^2$$

$$= \left|\sum_{i=0}^{N-1} a_i e^{ji\gamma'}\right|^2 \triangleq F_a(\gamma'), \tag{9.123}$$

where

$$\gamma' = kd\cos\theta - \delta. \tag{9.124}$$

For reasons that will become clear later, let us define the phase shift δ in terms of an angle θ_0, which we shall call the *scan angle*, as follows:

$$\delta = kd\cos\theta_0. \tag{9.125}$$

In this case, γ' becomes

$$\boxed{\gamma' = kd(\cos\theta - \cos\theta_0).} \tag{9.126}$$

The array factor given by Eq. (9.123) has the same functional form as the array factor developed earlier for the case of the uniform-phase array [see Eq. (9.113)], except that γ is replaced with γ'. Hence, *for any amplitude distribution across the array, the array factor of an array excited by a linear-phase distribution may be obtained from the expression developed for the array assuming a uniform-phase distribution simply by replacing γ with γ'.* For an amplitude distribution symmetrical with respect to the array center, the array factor $F_a(\gamma')$ is maximum when its argument $\gamma' = 0$. When the phase is uniform ($\delta = 0$), this condition corresponds to the direction $\theta = 90°$, which is why the uniform-phase case is called a broadside array. According to Eq. (9.126), in the more general case of a linearly phased array, $\gamma' = 0$ corresponds to $\theta = \theta_0$. Thus, by applying linear phase across the array, the array pattern is shifted along the $\cos\theta$-axis by an amount $\cos\theta_0$, and the direction of maximum radiation is *steered* from the broadside direction ($\theta = 90°$) to the direction $\theta = \theta_0$. To steer the beam all the way to the *end-fire* direction ($\theta = 0$), the incremental phase shift δ should be equal to kd radians.